Diastolic Spontaneous Calcium Release From the Sarcoplasmic Reticulum Increases Beat-to-Beat Variability of Repolarization in Canine Ventricular Myocytes After β-Adrenergic Stimulation

Daniel M. Johnson,* Jordi Heijman,* Elizabeth F. Bode, David J. Greensmith, Henk van der Linde, Najah Abi-Gerges, David A. Eisner, Andrew W. Trafford, Paul G.A. Volders

Rationale: **Spontaneous Ca^{2+} release (SCR) from the sarcoplasmic reticulum can cause delayed afterdepolarizations and triggered activity, contributing to arrhythmogenesis during β-adrenergic stimulation. Excessive beat-to-beat variability of repolarization duration (BVR) is a proarrhythmic marker. Previous research has shown that BVR is increased during intense β-adrenergic stimulation, leading to SCR.**

Objective: **We aimed to determine ionic mechanisms controlling BVR under these conditions.**

Methods and Results: **Membrane potentials and cell shortening or Ca^{2+} transients were recorded from isolated canine left ventricular myocytes in the presence of isoproterenol. Action-potential (AP) durations after delayed afterdepolarizations were significantly prolonged. Addition of slowly activating delayed rectifier K^+ current (I_{Ks}) blockade led to further AP prolongation after SCR, and this strongly correlated with exaggerated BVR. Suppressing SCR via inhibition of ryanodine receptors, Ca^{2+}/calmodulin-dependent protein kinase II inhibition, or by using Mg^{2+} or flecainide eliminated delayed afterdepolarizations and decreased BVR independent of effects on AP duration. Computational analyses and voltage-clamp experiments measuring L-type Ca^{2+} current (I_{CaL}) with and without previous SCR indicated that I_{CaL} was increased during Ca^{2+}-induced Ca^{2+} release after SCR, and this contributes to AP prolongation. Prolongation of QT, T_{peak}-T_{end} intervals, and left ventricular monophasic AP duration of beats after aftercontractions occurred before torsades de pointes in an in vivo dog model of drug-induced long-QT1 syndrome.**

Conclusions: **SCR contributes to increased BVR by interspersed prolongation of AP duration, which is exacerbated during I_{Ks} blockade. Attenuation of Ca^{2+}-induced Ca^{2+} release by SCR underlies AP prolongation via increased I_{CaL}. These data provide novel insights into arrhythmogenic mechanisms during β-adrenergic stimulation besides triggered activity and illustrate the importance of I_{Ks} function in preventing excessive BVR. (*Circ Res*. 2013;112:246-256.)**

Key Words: action potentials ■ arrhythmia ■ β-adrenergic receptors ■ calcium ■ sarcoplasmic reticulum

Enhanced cellular Ca^{2+} load, for example, during β-adrenergic receptor (βAR) stimulation, results in augmentation of Ca^{2+} release from the sarcoplasmic reticulum (SR), larger Ca^{2+} transients (CaT), and enhanced contractile force.[1] Under certain conditions, Ca^{2+} load is increased beyond a certain threshold, leading to spontaneous Ca^{2+} release (SCR) from the SR during diastole.[2] In turn, this diastolic leak causes a transient inward current (I_{ti}), causing delayed afterdepolarizations (DADs) mainly attributable to activation of the electrogenic Na^+-Ca^{2+} exchanger, with the Ca^{2+}-activated Cl^- current (I_{ClCa}) contributing in some species.[3,4] Previous work has shown that both DADs and early afterdepolarizations (EADs) may share a common mechanism, at least during βAR stimulation and Ca^{2+} overload, namely SCR-induced currents.[5] Both types of afterdepolarizations have been incriminated in the formation of ventricular tachycardia via triggered activity (TA) and by increasing dispersion of repolarization.[6]

Beat-to-beat variability (BVR) of repolarization duration occurs as an apparently random alteration in repolarization duration and can be observed at all levels from the action

Original received August 8, 2011; revision received November 5, 2012; accepted November 13, 2012. In October 2012, the average time from submission to first decision for all original research papers submitted to *Circulation Research* was 12.5 days.

From the Department of Cardiology, Cardiovascular Research Institute Maastricht, Maastricht University Medical Center, Maastricht, the Netherlands (D.M.J., J.H., P.G.A.V.); Department of Knowledge Engineering, Maastricht University, Maastricht, the Netherlands (J.H.); Unit of Cardiac Physiology, University of Manchester, Manchester, United Kingdom (E.F.B., D.J.G., D.A.E., A.W.T.); Center of Excellence for Cardiovascular Safety Research and Mechanistic Pharmacology, Janssen Research and Development, Beerse, Belgium (H.v.d.L.); and Department of Safety Pharmacology, Safety Assessment UK, AstraZeneca R&D, Alderley Park, Macclesfield, United Kingdom (N.A.-G.). J.H. is currently affiliated with Institute of Pharmacology, Medical Faculty Essen, University of Duisburg-Essen, Essen, Germany.

*These authors contributed equally to this work.

The online-only Data Supplement is available with this article at http://circres.ahajournals.org/lookup/suppl/doi:10.1161/CIRCRESAHA.112.275735/-/DC1.

Correspondence to Paul G.A. Volders, Department of Cardiology, Cardiovascular Research Institute Maastricht, Maastricht University Medical Center, P.O. Box 5800, 6202 AZ Maastricht, the Netherlands. E-mail p.volders@maastrichtuniversity.nl

Non-standard Abbreviations and Acronyms

AP	action potential
APD	action-potential duration
βAR	β-adrenergic receptor
BVR	beat-to-beat variability of repolarization duration
CaMKII	Ca^{2+}/calmodulin-dependent protein kinase II
CaT	Ca^{2+} transient
CDI	Ca^{2+}-dependent inactivation
CL	cycle length
DAD	delayed afterdepolarization
EAD	early afterdepolarization
ISO	isoproterenol
LQT1	long-QT syndrome type 1
LV	left ventricular
LV MAP	left ventricular monophasic action potential
RyR	ryanodine receptor
SR	sarcoplasmic reticulum
SCR	spontaneous Ca^{2+} release
TA	triggered activity
TdP	torsades de pointes
VT	ventricular tachycardia

potential (AP) of the single cardiac myocyte to the QT interval on the body surface.[7–9] Exaggerated BVR has been reported to be a more reliable indicator of arrhythmogenic risk than repolarization prolongation, per se, at least in several experimental ventricular tachycardia models[10–12] and in selected human subjects.[8,13]

Although BVR has been investigated in multiple studies, the mechanisms underlying this phenomenon at the single-cell level remain to be fully elucidated. Pharmacological interventions influencing ion channels that operate during the AP plateau can markedly alter BVR.[7,14] Despite the fact that inhibition of the slowly activating delayed rectifier K^+ current (I_{Ks}) alone has minimal effects on both cellular AP duration (APD) and BVR,[14] we recently have shown that during increased Ca^{2+} loading in myocytes subjected to blockade of I_{Ks} in combination with βAR stimulation, BVR is significantly enhanced, even before the occurrence of EADs and TA.[14]

In the present study, we investigated the relationship between SCR and BVR using a combined experimental and computational approach in both canine ventricular myocytes and in situ hearts subjected to βAR stimulation. We show that SCRs not only lead to I_{ti} and DAD formation but also lead to a prolonged duration of AP via increased L-type Ca^{2+} current (I_{CaL}), which in turn leads to increased BVR when analyzing multiple consecutive APs. Pharmacological interventions that inhibit SCR (either with reduced or with preserved systolic contraction) prevent this SCR-associated AP prolongation and reduce BVR.

Methods

This investigation conformed to the Guide for the Care and Use of Laboratory Animals published by the United States National Institutes of Health (National Institutes of Health Publication 85-23, revised 1996). Animal handling was in accordance with the European Directive for the Protection of Vertebrate Animals Used for Experimental and Other Scientific Purposes (86/609/EU). Full details of methods, solutions, and interventions used are given in the online-only Data Supplement accompanying this article. A brief summary of the main aspects is provided.

Myocyte Isolation and Electrophysiology

Canine left ventricular (LV) myocytes were isolated as previously described.[15] Transmembrane APs were recorded at ≈37°C using high-resistance (30–60 MΩ) glass microelectrodes filled with 3 mol/L KCl. Myocyte contractions were recorded with a video edge motion detector.

Calcium Measurement

We used the perforated patch-clamp technique under current-clamp or voltage-clamp control as previously described.[16] Myocytes were stimulated to elicit APs (current clamp) or I_{CaL} (voltage clamp). Changes in intracellular Ca^{2+} concentration ($[Ca^{2+}]_i$) were measured using Fluo-3 or Fura-2 AM.[16]

Computational Analysis

A recent model of the canine ventricular myocyte electrophysiology including βAR stimulation[17] was extended with a method to induce diastolic SR Ca^{2+} release in 1 of 2 identical Ca^{2+} domains in a controlled fashion (Online Figures I and II). Simulations were performed in single cells as well as in a 1-dimensional homogeneous strand or 2-dimensional tissue of electrically coupled cells to determine the effects of diastolic Ca^{2+} release in the presence of electrotonic coupling.

In Vivo Dog Model of Drug-Induced Long-QT1 Syndrome

Torsades de Pointes (TdP) arrhythmias were induced in an in vivo dog model of long-QT1 (LQT1) syndrome as previously described.[11] ECG, LV pressure, and LV monophasic APs (LV MAPs) were recorded throughout the experiments and analyzed offline.

Data Analysis and Statistical Comparisons

APD was quantified at 90% repolarization. BVR was quantified as variability of APD using the formula $\sum\left(\left|APD_{i+1}-APD_i\right|\right)/[n_{beats}\times\sqrt{2}]$ for 30 consecutive APs in the absence of TA.[10] DADs were detected with a semiautomated method using a custom software script (online-only Data Supplement). When applicable, data were reported as mean±SEM of number experiments and significance was tested with either *t* test or 1-way ANOVA. Differences were considered statistically significant if $P<0.05$.

Results

DADs Prolong Subsequent APs and Increase BVR

Under baseline conditions, a small beat-to-beat APD variability was observed (Figure 1A, left). βAR stimulation with isoproterenol (ISO) shortened APD and enhanced contraction (Figure 1A, middle). In the majority of cells, 100 nmol/L ISO caused DADs during pacing at 1000-ms cycle length (CL). APs after a DAD were prolonged, leading to increased BVR attributable to interspersed occurrence of normal and prolonged APs (Figure 1A, middle). Pharmacological inhibition of I_{Ks} by HMR1556 (500 nmol/L) in the presence of ISO further prolonged APD and increased BVR (Figure 1A, right). In separate experiments, CaT were recorded together with APs after HMR1556 and ISO. HMR1556 alone did not increase the CaT amplitude or lead to any SCR events. The combination of HMR1556 and ISO, however, led to large increases in CaT amplitude and SCR, as expected.[18] APs after SCR were prolonged and had a reduced systolic CaT amplitude compared with those in which no diastolic release preceded the AP, indicating reduced SR Ca^{2+} load at the start of the AP (Figure 1B), consistent with the reduced cell shortening after an aftercontraction (Figure 1A).

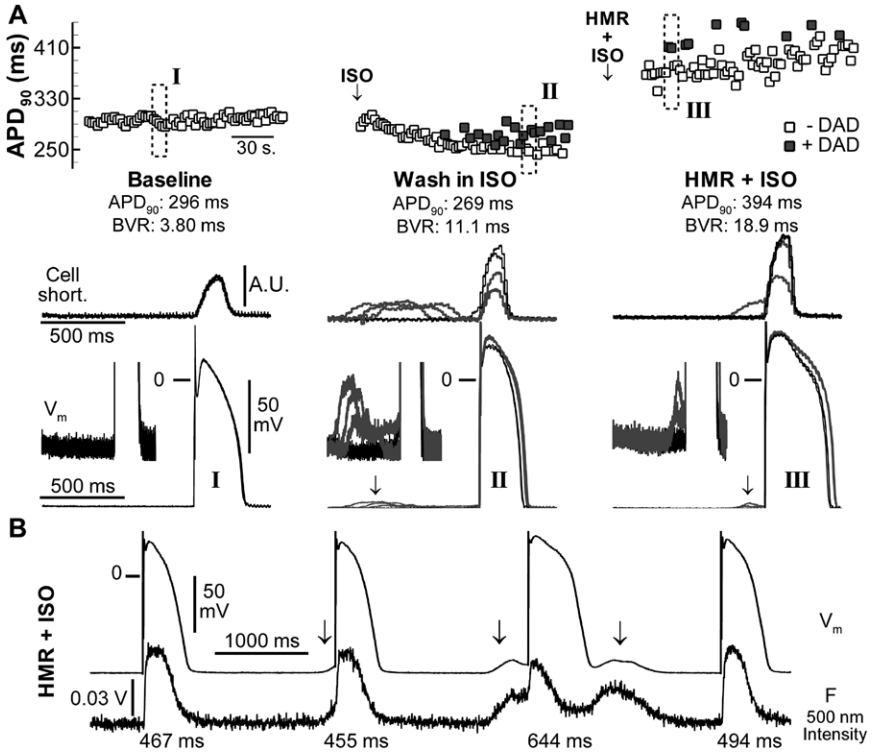

Figure 1. Occurrence of delayed afterdepolarizations (DADs) in canine ventricular myocytes is associated with prolongation of subsequent action potentials (APs) and increased beat-to-beat variability (BVR) of repolarization duration. A, AP duration (ADP_{90}) for 75 consecutive beats at 2000-ms cycle length (CL) at baseline (**left**: I), during wash-in of isoproterenol (ISO) (**middle**: II), and in the presence of HMR1556 and ISO (**right**: III). APDs preceded by DAD are indicated with filled symbols, APDs without DADs are depicted by open symbols. Dashed rectangle indicates a set of 5 beats for which cell shortening and membrane potential are depicted below. Insets show diastolic potentials at an expanded scale. Beats without previous spontaneous Ca^{2+} release (SCR) are indicated in black; beats with previous SCR are depicted in gray. **B,** Membrane potential (**top**) and $[Ca^{2+}]_i$ for 4 consecutive beats. APD_{90} is indicated below each AP. SCR is indicated with **arrows.**

APD prolongation after a DAD was significantly more pronounced in the presence of ISO plus HMR1556 compared with ISO alone at all CLs (eg, 41±6 ms vs 15±4 ms at CL=1000 ms; $P<0.05$; Figure 2A), and this coincided with a significant increase in BVR (17±2 ms vs 7±1 ms; $P<0.05$; Figure 2B). As such, HMR1556 was added in all subsequent experiments in the presence of ISO to maximize effects on APD, essentially creating a cellular model of drug-induced LQT1 syndrome.[14] DADs showed typical rate-dependent properties, including increased amplitude and decreased AP–DAD coupling interval at shorter pacing CL, consistent with previous results.[19] I_{Ks} blockade did not alter rate-dependent DAD properties (Online Figure III).

To determine whether DAD-like membrane-potential changes alone (ie, without underlying alterations in intracellular Ca^{2+}) influenced the subsequent AP, current was injected to induce small alterations in the resting membrane potential (25-mV amplitude, 150-ms duration; Figure 2C, top). There was no significant difference between APDs in the absence or presence of these diastolic pulses (Figure 2D), independent of the timing of the pulse (not shown). In contrast, when these cells were stimulated with HMR1556 plus ISO, DADs occurred and subsequent APD was significantly prolonged (Figure 2C, bottom), indicating that alterations in the subsequent APD were influenced by DAD-related events other than membrane-potential alterations per se.

Coupling Between the Occurrence of DADs and EADs During β-Adrenergic Stimulation and I_{Ks} Blockade

In addition to DADs, EADs were observed. EADs occurred predominantly at 500-ms CL and exclusively in the presence of HMR1556 plus ISO. We observed early aftercontractions preceding EAD upstrokes by 21±5 ms (Figure 3A and 3C),[5] consistent with the observations by Zhao et al[20] in rabbit ventricular myocytes challenged with ISO and the I_{CaL} agonist Bay K 8644, suggesting a role of SCR for EAD formation under these specific conditions.[5] We quantified the occurrence of DADs in the beats preceding an EAD and found that DADs were significantly more likely to occur in the 2 beats directly preceding an EAD (53% and 95% of APs) compared with average DAD occurrence for all beats (34%; Figure 3A, bottom). Figure 3B shows the responses during ISO alone.

Blockade of Spontaneous SR Ca^{2+} Release Reduces BVR

We sought to further investigate how eliminating SCR would affect APD and BVR. Blockade of the ryanodine receptor (RyR) with ryanodine eliminated DADs and led to a drastic reduction in BVR, despite leading to an increased APD (Figure 4A and 4B). APD prolongation under these conditions was not associated with any arrhythmogenic events. A drastic

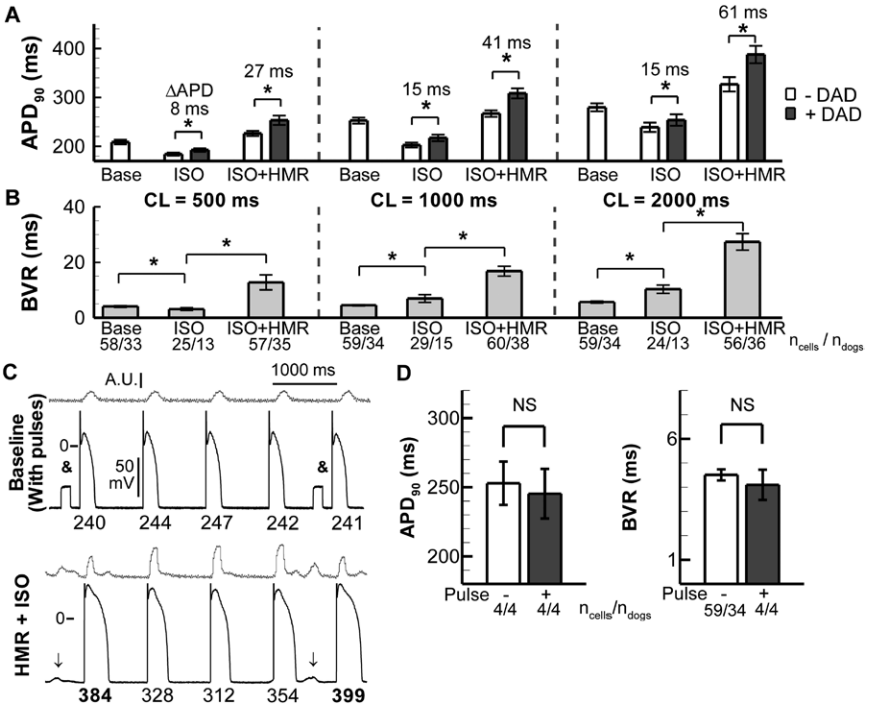

Figure 2. A, Group data for action-potential duration (ADP_{90}) under baseline conditions, in the presence of isoproterenol (ISO), or in the presence of ISO plus HMR1556 at cycle lengths (CLs) of 500, 1000, and 2000 ms. Delayed afterdepolarizations (DADs) cause a significant prolongation during ISO and ISO plus HMR1556 treatment. APD_{90} differences are indicated above each pair of bars. *P<0.05 based on paired t test. **B,** Beat-to-beat variability (BVR) of repolarization duration values for the conditions in (**A**). The number of cells and number of dogs for each condition are indicated below each bar. Comparisons between conditions were made using ANOVA. **C,** Cell shortening (**top trace**) and membrane potential (**bottom trace**) under baseline conditions with DAD-like electric pulses (in the absence of spontaneous Ca^{2+} release [SCR]) applied every fourth beat (**top**) or with DADs after ISO plus HMR1556 in the same cell (**bottom**). APD_{90} is indicated below each beat. **D,** Subthreshold diastolic pulses do not alter APD_{90} within the same cell (**left**) or BVR compared with cells without diastolic pulses (**right**).

reduction in systolic contraction was also seen, as expected, indicating that blockade of RyRs was achieved effectively.

Tetracaine reduces the open probability (P_o) of RyR, leading to a decrease in the frequency of SCR in unstimulated rat ventricular myocytes[21] and the abolishment of ISO-induced SCR in voltage-clamped rat ventricular myocytes.[22] Similar to ryanodine, tetracaine led to an elimination of DADs in our experiments and a reduction in BVR at all CLs. However, unlike ryanodine, cell shortening remained largely unaltered, indicating that systolic Ca^{2+} release was largely intact (Figure 4C and 4D).

To determine the effects of increasing the P_o of RyRs, as opposed to decreasing it, we used low concentrations of caffeine (maximally 500 μmol/L).[23] Under these conditions, the percentage of APs showing DADs was increased at all CLs. Interestingly, this led to a significant decrease in BVR compared with HMR1556 and ISO alone, because DADs occurred before every AP (Figure 5, rightmost grey bars).

Several studies have shown that Ca^{2+}/CaMKII is an important signaling molecule affecting Ca^{2+}-induced Ca^{2+} release and that its inhibition can be antiarrhythmic.[24] Curran et al[25] demonstrated that SR Ca^{2+} leak during βAR stimulation is mediated by Ca^{2+}/calmodulin-dependent protein kinase II (CaMKII). In our experiments, inhibition of calmodulin using W7 reduced DAD incidence in all cells (from 44% to 8% at 1000 ms CL; P<0.05) and completely abolished them in 3 of 7 cells. The decrease in DAD occurrence was paralleled by a decrease in BVR. Average APD was unaltered by W7, and systolic contractions remained intact. Application of the CaMKII inhibitor KN93 led to similar results (Figure 5, black bars).

Mg^{2+} has been shown to suppress both EADs and DADs in different models[26,27] and is used clinically as a first-line agent against TdP. Increasing extracellular [Mg^{2+}] from 1 mmol/L to 5 mmol/L abolished DADs induced after HMR1556 and ISO in 4 of 7 cells. In the remaining 3 cells, DAD incidence was significantly reduced. A concomitant reduction in BVR was seen. APDs were not significantly altered, and although systolic contractions were slightly reduced compared with beats that did not show SCR events before Mg^{2+} they remained stable, suggesting that the SR content remained constant (not shown). Similar results (albeit with reduced APD) were obtained with the class IC antiarrhythmic agent flecainide (Figure 5, striped bars), which has been shown to be effective in preventing catecholaminergic polymorphic ventricular tachycardia because of its effects on RyR and Na^+ channels.[28]

Increases in $[Ca^{2+}]_o$ Can Reinstate SCR Only When Residual RyR Function Is Available

We hypothesized that increases in $[Ca^{2+}]_o$ after interventions that reduced DAD occurrence would lead to recurrence of SCR and DADs and increase BVR. Therefore, we raised the $[Ca^{2+}]_o$ from 1.8 mmol/L to 3.6 mmol/L after application of ryanodine, tetracaine, or W7. This led to a reinduction of DADs after tetracaine or W7, and to a significant decrease of

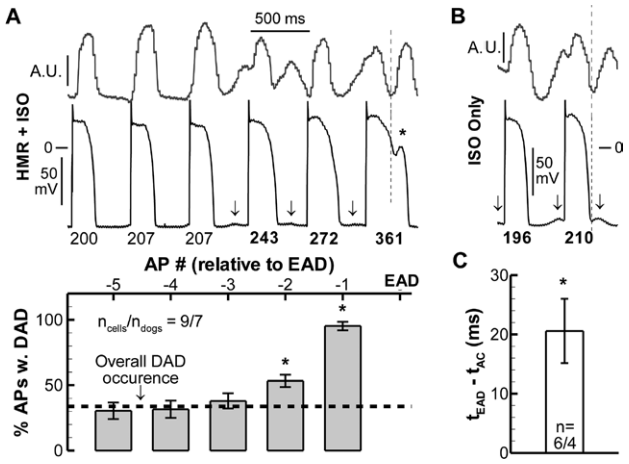

Figure 3. Relationship between diastolic spontaneous Ca^{2+} release (SCR) and early afterdepolarizations (EADs). **A**, Cell shortening (**top trace**) and membrane potential (**bottom trace**) for 5 consecutive action potentials (APs) followed by an AP with EAD (indicated with *) in a representative cell at 500-ms cycle length (CL) in the presence of HMR1556 plus isoproterenol (ISO). AP duration $(APD)_{90}$ is given below each beat and delayed afterdepolarizations (DADs) are indicated with **arrows**. Vertical line indicates start of aftercontraction. **Bottom** indicates the percentages of APs that showed a DAD in the 5 beats preceding every EAD. Horizontal dashed line indicates overall DAD occurrence at 500-ms CL in the presence of HMR1556 plus ISO, independent of EADs. The beat before an EAD has a DAD 95% of the time. *P<0.05 compared with overall DAD occurrence. **B,** Similar to (**A**, **top**) for 2 beats in the presence of ISO only. A similar contraction pattern can be observed, but APD prolongation is insufficient to promote EAD formation. **C,** Time differences between increase of aftercontraction and EAD, indicating that aftercontractions initiate earlier than EADs.

APD (Online Figure IVA–IVC). However, increasing $[Ca^{2+}]_o$ after ryanodine did not lead to DADs, nor did it alter BVR, indicating that RyR function is required for SCR, and without this BVR cannot be altered. Interestingly, BVR was not significantly reincreased after W7 and high $[Ca^{2+}]_o$, whereas after tetracaine and high $[Ca^{2+}]_o$ it was, despite DADs being reinstated under both conditions (Online Figure IVB and IVC). In the presence of W7, APs after SCR were no longer prolonged (Online Figure IVC, inset). These data suggest that calmodulin inhibition has a direct effect on the coupling between SCR and APD, possibly via I_{CaL}.

Reduced Ca^{2+}-Dependent Inactivation of I_{CaL} Underlies APD Prolongation After SCR

We used a computational model of the canine ventricular myocyte[17] to further investigate the ionic basis of the coupling between SCR and APD prolongation. After pacing to steady-state, a partial release of SR Ca^{2+} was induced during diastole. After this release, APD was prolonged, consistent with experimental observations (Figure 6A; 1000-ms CL in the presence of ISO). The prolonged APD was associated with a decreased CaT, an increase in the sustained component of I_{CaL}, and increased I_{Ks}. The increase in I_{Ks} was attributable to the increased plateau potential resulting from the larger I_{CaL} and it counteracted the repolarization delay. As such, APD prolongation was significantly larger when I_{Ks} was inhibited (Figure 6B). An increase in plateau V_m also was observed in experimental recordings (maximum amplitude of plateau was 114±1 mV without previous DAD and 118±1 mV after DADs at 1000 ms CL in the presence of HMR1556 plus ISO; P<0.05).

Several currents underlying the ventricular AP are modified by intracellular Ca^{2+}. To determine the relative contribution of each component, we used the model to selectively inhibit each current for 1 final beat at steady-state after either a normal diastole or SCR. Inhibition of the main currents activated by SCR in the dog (I_{NaCa} and I_{ClCa})[3,29] only had a minor impact on the APD differences in the presence and absence of SCR (Figure 6C). In contrast, inhibition of I_{CaL} or RyR was able to significantly reduce DAD-provoked APD prolongation. More specifically, when only Ca^{2+}-dependent inactivation (CDI) of I_{CaL} was inhibited, APD after SCR was no longer prolonged compared with APD without previous SCR (Figure 6C). Further investigation showed any differences in APD in these conditions were because of priming of CDI attributable to a transition of L-type Ca^{2+} channels to the Ca^{2+}-dependent tier of the Markov model induced by the Ca^{2+} that was released during the SCR, before activation of inhibition.

Combined, our data implicate reduced SR Ca^{2+}-release-dependent inactivation of I_{CaL} as the mechanism underlying APD prolongation after SCR. This prediction was confirmed under voltage-clamp conditions in native canine ventricular myocytes when the extracellular solution was modified to isolate I_{CaL} (Figure 7). During a voltage step to +10 mV from a holding potential of −80 mV, a significant increase in the integral of I_{CaL} was observed after SCR: $\int I_{CaL}$=27.9±3.5 nC vs 33.0±3.5 nC in the absence or presence of SCR, respectively (P<0.05).

Relation Between Aftercontractions, Repolarization Prolongation, and Dispersion and Arrhythmogenesis in the Intact Canine Heart

To evaluate whether the single-cell mechanisms described above could affect arrhythmogenesis in vivo, we used a canine model of drug-induced LQT1.[11] Application of a bolus of ISO during continuous HMR1556 infusion resulted in aftercontractions exclusively in the LV pressure signal before the development of ventricular premature beats and TdP (Figure 8A). In parallel with the occurrence of aftercontractions, we observed paradoxical QT prolongation during β-adrenergic heart rate acceleration, resulting in a significant increase of the QT interval in the last sinus beats before the extrasystoles triggering TdP (Figure 8B). Similarly, LV MAP duration was significantly prolonged in these beats and a significant increase in T_{peak}-T_{end} interval was noted (Figure 8B), which could reflect an increased dispersion of repolarization. We focused on repolarization duration by comparing the beats before and after the first notable aftercontraction. QT, LV MAP, and T_{peak}-T_{end} durations were significantly increased in the beat after the first aftercontraction, whereas the RR intervals were unchanged (Figure 8C). Furthermore, the I_{CaL} inhibitor verapamil (0.4 mg/kg) prevented TdP induction by ISO during continuous HMR1556 infusion in 5 of 5 animals (Figure 8A), although some ventricular extrasystolic activity still could be observed (Online Figure VIII). Similar chronotropic responses were seen after ISO in the presence of verapamil but, in the absence of aftercontractions, QT, LV MAP, and T_{peak}-T_{end} prolongation were significantly smaller when compared with HMR1556

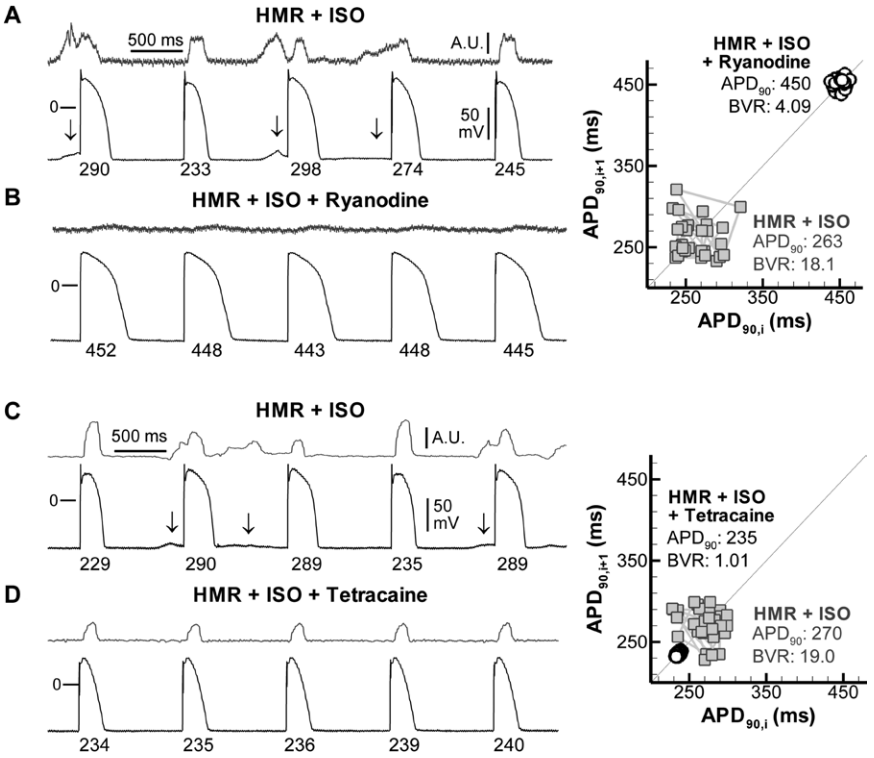

Figure 4. Inhibition of (diastolic) spontaneous Ca^{2+} release (SCR) abolishes delayed afterdepolarizations (DADs) and reduces beat-to-beat variability (BVR) of repolarization duration. Cell shortening (**top**; arbitrary units) and membrane potential (**bottom**) for 5 representative beats during treatment with isoproterenol (ISO) plus HMR1556 (**A**) or ISO plus HMR1556 plus ryanodine (1 μmol/L) (**B**). Action-potential duration (ADP_{90}) is indicated below each beat and mean APD_{90} and BVR are shown for 30 beats in the Poincaré plot on the right. DADs are indicated with **arrows**. **C** and **D,** Similar data for treatment with tetracaine (5 μmol/L). ISO plus HMR1556 enhances BVR and DAD occurrence. Ryanodine and tetracaine abolish DADs and reduce BVR.

and ISO alone (Figure 8B). These data illustrate the role of Ca^{2+}-dependent regional repolarization prolongation for TdP induction in this model.

To further test the hypothesis that SCR at the single-myocyte level can contribute to the QT and T_{peak}-T_{end} interval prolongation seen in vivo, we performed computer simulations of both a homogeneous 1-dimensional strand and a 2-dimensional tissue of electrically coupled myocytes. Consistent with our hypothesis, diastolic SR Ca^{2+} release increased repolarization duration and spatial dispersion of repolarization in both simulations (Figure 8D, Online Figures V–VI), and this effect was completely abolished by inhibition of I_{CaL} CDI (Figure 8D, Online Figure VII).

Discussion

In this study, we elucidated the relationship between SCR, AP prolongation, and BVR in canine LV myocytes and provide arguments for its arrhythmogenic significance in the in vivo beating heart. Our data indicate that under conditions of ISO-induced Ca^{2+} loading, SCR can occur over a wide range of pacing CLs and that APD after SCR is significantly prolonged. Reduced Ca^{2+}-induced Ca^{2+} release-dependent inactivation of I_{CaL} after SCR is involved in this AP prolongation. The increase in BVR was strongly dependent on the degree of APD prolongation after SCR. In anesthetized dogs subjected to similar conditions, we observed the occurrence of mounting aftercontractions in parallel with QT, T_{peak}-T_{end}, and LV MAP prolongation just before TdP, which could be prevented by inhibition of I_{CaL} and Ca^{2+} load with verapamil. SCR-related repolarization prolongation was reproduced in multicellular computer simulations. Our data align with recent data showing that local βAR stimulation synchronizes SCR in the normal rabbit heart, leading to Ca^{2+}-mediated focal arrhythmia.[30] In the setting of exaggerated spatio-temporal dispersion of repolarization, such focal activity may trigger TdP, as actually observed in the canine model of drug-induced LQT1 syndrome and βAR stimulation.[11]

Previous cellular studies[31,32] have shown that large CaTs result in abbreviation of APD, whereas a small CaT after SR Ca^{2+} depletion corresponds to prolonged APD. In agreement, we found substantial APD prolongation after application of ryanodine because of reduced CDI of I_{CaL}. Furthermore, I_{CaL} CDI is sensitive to (partial) SR Ca^{2+} unloading by SCR. These changes in CDI are sufficient to modulate APD on a beat-to-beat basis over a wide range of CLs. Interestingly, Spencer and Sham reported the opposite effect in guinea pig ventricular myocytes, perhaps because of species differences in the balance of Na^+-Ca^{2+} exchanger and I_{CaL}.[33] In the present study, we used Ca^{2+}-sensitive fluorescent probes and cell shortening as Ca^{2+} indicators. Both measures reflect cytosolic Ca^{2+} levels, which are substantially different from the subsarcolemmal $[Ca^{2+}]$ influencing Ca^{2+}-activated membrane currents.

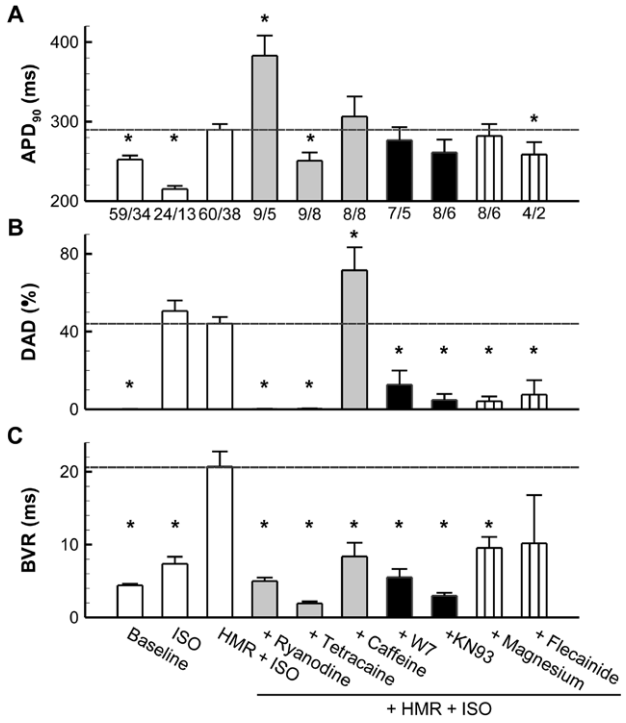

Figure 5. Interventions that abolish or homogenize spontaneous Ca^{2+} release (SCR) lower beat-to-beat variability of repolarization (BVR) duration. A, Action-potential duration (ADP_{90}). The n_{cells}/n_{dogs} are indicated below each bar. **B,** Delayed afterdepolarization (DAD) occurrence. **C,** BVR at cycle length (CL)=1000 ms at baseline and in the presence of isoproterenol (ISO), HMR1556 plus ISO, or HMR1556 plus ISO combined with interventions to modulate SCR. Interventions are grouped by type (ryanodine receptor [RyR] modulation, grey; Calmodulin/Ca^{2+}/calmodulin-dependent protein kinase II modulation, black; or agents also used clinically, striped). All interventions except caffeine result in a significant lowering of DAD incidence and a concomitant reduction of BVR, with increased (ryanodine), decreased (tetracaine, flecainide [6 μmol/L]), or unaltered (W7 [1 μmol/L], KN93 [5 μmol/L], [Mg^{2+}] [5 mmol/L]) APD_{90}. Caffeine (maximally 500 μmol/L) homogenizes SCR occurrence, increasing DAD occurrence but lowering BVR without changing APD_{90}. *P<0.05 vs HMR1556 plus ISO.

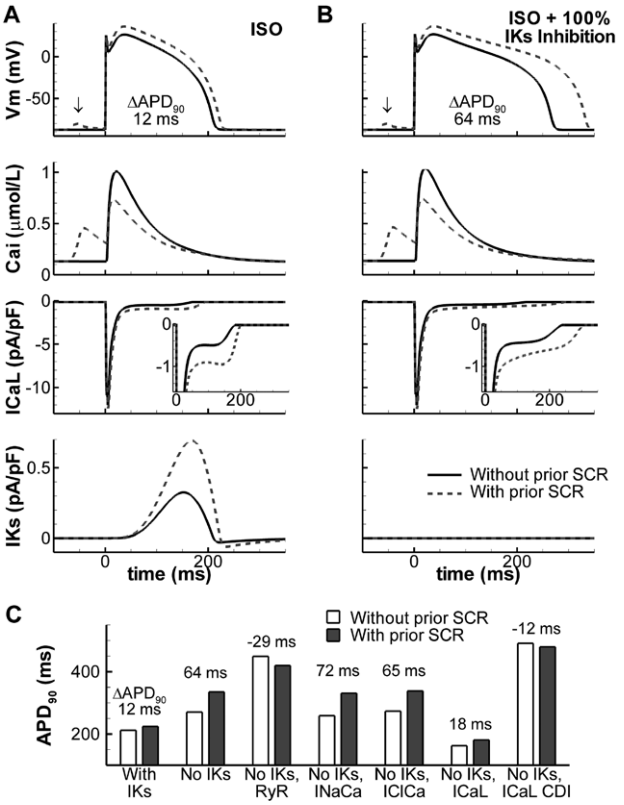

Figure 6. Computational model of the canine ventricular myocyte implicates reduced sarcoplasmic reticulum (SR) Ca^{2+}-dependent inactivation (CDI) of L-type Ca^{2+} current (I_{CaL}) to cause action-potential duration (APD) prolongation. A, Action potential (AP), intracellular Ca^{2+}, I_{CaL}, and delayed-rectifier K^+ current (I_{Ks}) (**top to bottom**) with (**dashed lined**) or without (solid lines) previous SR Ca^{2+} release for a single beat after pacing to steady-state in the presence of isoproterenol (ISO) at cycle length (CL) of 1000 ms. The delayed afterdepolarization (DAD) resulting from the spontaneous Ca^{2+} release (SCR) is indicated by an **arrow**. Inset in third panel shows I_{CaL} during AP plateau on an expanded scale. **B**, Similar to (**A**) in the presence of ISO and complete inhibition of I_{Ks}. **C**, After pacing to steady-state in the presence of ISO, SCR was triggered (shaded bars) or not (white bars) and individual currents/fluxes were blocked for 1 final beat. APD_{90} differences are indicated above each bar. Only inhibition of SR Ca^{2+} release (ryanodine receptor [RyR]) or I_{CaL} CDI was sufficient to abolish the APD prolongation after SCR.

The Importance of I_{Ks} Blockade

Burashnikov and Antzelevitch[34] demonstrated that I_{Ks} block alone was insufficient to induce DADs or to modulate repolarization heterogeneity in canine transmural ventricular tissues.[34] However, it amplified the effects of adrenergic stimuli. At the myocyte level, we previously have shown that I_{Ks} blockade (via KCNQ1 inhibition)[35] has minimal effects on APD and BVR under baseline conditions. During βAR stimulation and I_{Ks} blockade, BVR is significantly increased and this is, at least partly, dependent on $[Ca^{2+}]_i$.[14] Here, we extend this by determining an important role for CDI of I_{CaL}, at least in the presence of SCR. Under baseline conditions, rapidly activating delayed-rectifier K^+ current (I_{Kr}) is the main repolarizing current in canine ventricular myocytes and inhibition of I_{Kr} can cause EADs attributable to APD prolongation and subsequent I_{CaL} reactivation.[14] During additional βAR stimulation, the balance of the repolarization reserve is altered and the role of I_{Ks} becomes more prominent; enhanced I_{Ks} prevents repolarization instability and EAD generation by other proarrhythmic mechanisms (eg, I_{Kr} inhibition or augmentation of late I_{Na}). In contrast, inhibition of I_{Ks} during βAR stimulation leads to APD prolongation and increased BVR and EADs, indicating that under our conditions with βAR stimulation, I_{Ks} is a major contributor to repolarization. Bárándi et al[36] previously have shown that the degree of APD prolongation induced by pharmacological block of repolarizing currents or augmentation of depolarizing currents depends on baseline APD. Consistent with these results, we found a more pronounced APD prolongation after SCR at slow CL and in the presence of I_{Ks} blockade. In our experiments, APD prolongation after SCR is particularly pronounced because the increase in I_{CaL} also elevates the plateau potential, which increases I_{Ks} activation and offsets the prolongation induced by I_{CaL} (Figure 6A, bottom). This compensating mechanism is absent when I_{Ks} is inhibited. Thus, I_{Ks} inhibition exacerbates the effect of SCR on APD prolongation.

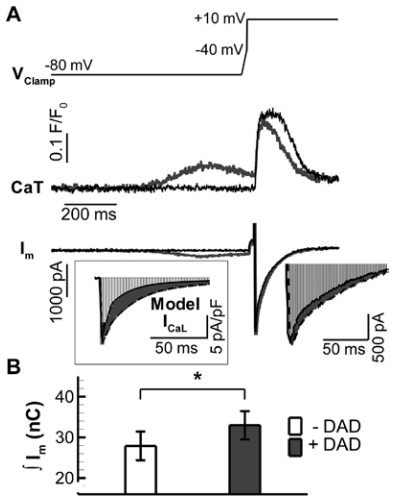

Figure 7. L-type Ca^{2+} current (I_{CaL}) inactivation is slowed after spontaneous Ca^{2+} release (SCR). A, Voltage-clamp protocol (**top**), intracellular Ca^{2+} (**middle**), and membrane current (**bottom**) in a representative canine ventricular myocyte in the presence of HMR1556 plus isoproterenol (ISO) plus increased $[Ca^{2+}]_o$ (3.6 or 5.0 mmol/L) in the absence (black) or presence of previous SCR (gray). **Right** inset shows membrane current at an expanded scale. 4-AP (5.0 mmol/L) and $BaCl_2$ (0.1 mmol/L) were used to isolate I_{CaL}. **Left** inset shows model results under similar conditions. **B**, Quantification of average membrane current integral (shaded area in **right** inset of **A**) in 6 canine ventricular myocytes in the absence or presence of SCR. Previous SCR significantly increases total inward current (*P<0.05).

The Role of SCR in Arrhythmogenesis

It has long been established that SCR-induced TA is a major arrhythmogenic mechanism during Ca^{2+} overload and its occurrence is increased in various pathological conditions.[6,37] Here, we observed that diastolic SCR prolongs the subsequent APD, suggesting that even SCR below the threshold for TA has important electrophysiological effects that may be proarrhythmic. Regional prolongation of APD after SCR in the intact heart may cause increased spatial dispersion of repolarization between regions with the highest Ca^{2+} load (generating SCR) and regions with lower Ca^{2+} loading. In agreement with this hypothesis, we observed increased QT duration and T_{peak}-T_{end} intervals after the first aftercontraction on a challenge with a bolus of ISO during I_{Ks} blockade in vivo. Regional heterogeneities in ion channel expression or intercellular conduction may further amplify this dispersion. Combined, these mechanisms can promote functional reentry. Stabilization of Ca^{2+} handling therefore may not only reduce the incidence of arrhythmogenic triggers but also prevent their reentrant perpetuation. Although current pharmacological interventions do not allow specific targeting of SCR or measurement of cellular Ca^{2+} handling in the in vivo dog heart, we found that I_{CaL} inhibition with verapamil could prevent aftercontractions and TdP in our model of LQT1, and this was associated with a reduction in the paradoxical increase in QT and T_{peak}-T_{end} intervals after ISO.

We also have shown that the combination of ISO and fast pacing can give rise to diastolic SCR, which prolongs APD sufficiently such that the next SCR occurs before the end of repolarization, generating an EAD. The common dependence of DADs and EADs on SCR in the presence of ISO previously has been described[5,19] and is in agreement with recent findings in rabbit ventricular myocytes.[20]

Our results provide novel mechanistic insights on the coupling between SCR, APD prolongation, and EAD occurrence, and illustrate that diastolic SCR is a central element in both TA and repolarization instability. However, the ionic mechanisms of EAD generation, particularly the relative roles of I_{NCX} and I_{CaL}, are complex and cannot be fully determined based on our data. Moreover, the measurement of the lag between the start of the aftercontraction and the EAD upstroke does not take into account the delay between SCR and activation of contraction or the SCR-induced slowing of repolarization in the priming phase before the EAD upstroke. This lag is likely because of differential Ca^{2+} thresholds for the activation of contraction vs the activation of membrane currents.

APD prolongation after SCR results from increased I_{CaL}, which enhances Ca^{2+} loading via increased sarcolemmal Ca^{2+} influx. Enhanced loading along with reduced Ca^{2+} efflux serves to restore and fine-tune SR Ca^{2+} content to maintain Ca^{2+}-induced Ca^{2+} release efficacy, as previously has been described in rat ventricular myocytes.[31,32] However, during increased Ca^{2+} load, these mechanisms will readjust, promoting SCR, facilitating the occurrence of afterdepolarizations. Consistent with this, we found that the probability of observing a DAD was not significantly altered by the presence of a DAD on the previous beat. This strongly implies that under our experimental conditions, the reduction in myocyte Ca^{2+} load during a DAD is overcome by the increased sarcolemmal Ca^{2+} influx during the following prolonged AP. Thus, APD prolongation after SCR contributes to the vicious cycle of Ca^{2+} loading and, ultimately, overload. These results are in agreement with the recent modeling study by Morotti et al[38] that established that I_{CaL} predominantly inactivates because of CDI and that (strongly) reduced CDI can cause Ca^{2+} overload and DADs.

Inhibition of SCR by ryanodine and tetracaine previously has been described,[19,22] and the results presented here agree with those data. We extend these observations by showing a concomitant decrease in BVR. Both ryanodine and tetracaine are useful for mechanistic studies, but because of their deleterious effects in vivo they cannot be used as therapeutic agents. In contrast, both magnesium and flecainide are commonly used antiarrhythmic agents. Here, we show that both these agents can lead to a reduction in BVR and arrhythmogenic events, most likely because of stabilization of Ca^{2+} handling in the single myocyte. Similarly, we confirm the usefulness of modulating Calmodulin/CaMKII during increased Ca^{2+} loading as an antiarrhythmic strategy.[24] CaMKII phosphorylation has been shown to induce a different gating mode (mode 2) of the I_{CaL} channel, thereby reducing inactivation and favoring Ca^{2+} entry and the occurrence of EADs and DADs.[39] Interestingly, when CAMKII inhibition is applied, a disconnect appears between SCR events and APD. Whether this is attributable to alterations in CDI or because of effects on other CAMKII substrates, such as I_{NaL}, is not clear and further investigation is warranted. In this regard, the development of selective CaMKII modulators suitable for antiarrhythmic interventions in humans is awaited.

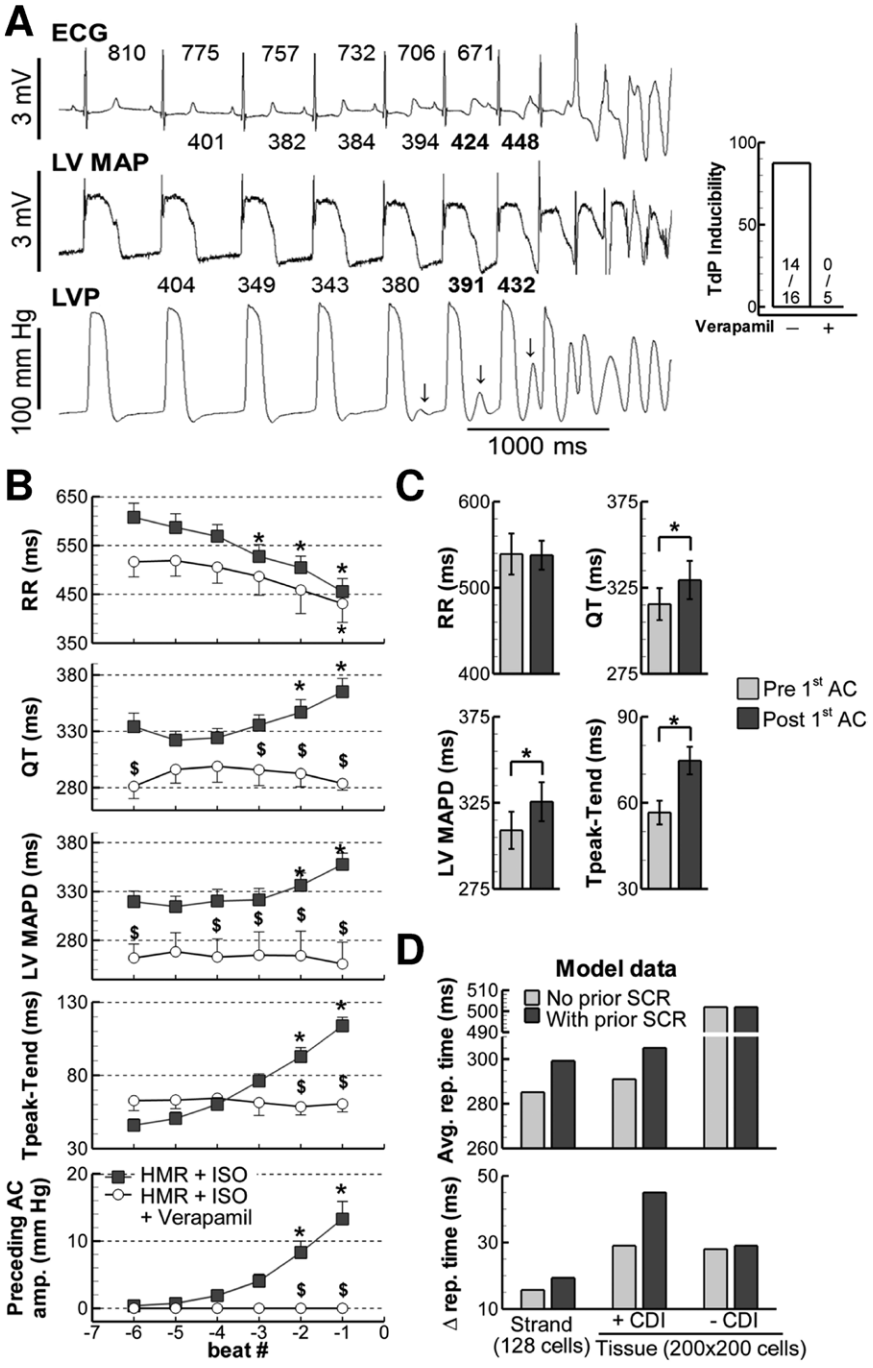

Figure 8. Aftercontractions (AC) and repolarization prolongation precede the occurrence of Torsades de pointes (TdP) in an in vivo canine model of long-QT syndrome type 1 (LQT1). A, ECG, left ventricular monophasic action potential (LV MAPs), and left ventricular pressure (LVP) in the 6 beats before the first extrasystolic beat and initiation of TdP in a representative experiment after a bolus of isoproterenol (ISO) in the presence of HMR1556. Inset shows TdP inducibility by ISO during HMR1556 in the absence or presence of verapamil. **B,** Group data showing electrophysiological properties (RR interval, QT interval, LV MAP duration, and T_{peak}–T_{end} interval) and average amplitude of the preceding aftercontraction in the absence (filled squares; n=14) or presence (open circles; n=5) of verapamil. **P*<0.05 compared with beat 6 (ANOVA for repeated measures with Bonferroni post hoc test). $*P*<0.05 vs the absence of verapamil for the same beat. Data are shown relative to the start of TdP or during the maximal chronotropic response to ISO. **C,** Comparison of the electrophysiological properties of the beats preceding (light grey) and after (dark grey) the first aftercontraction during HMR plus ISO: RR interval, QT interval, LV MAP duration, and T_{peak}–T_{end} interval. **P*<0.05 compared with before the first AC. **D,** Effect of diastolic Ca^{2+} release in 25% of the cells on average repolarization time (**top**) and spatial dispersion of repolarization (**bottom**) in 1-dimensional strand simulations and 2-dimensional tissue simulations with intact or disabled L-type Ca^{2+} current (I_{CaL}) Ca^{2+}-dependent inactivation (CDI).

Conclusions

We have shown that after SCR, inactivating I_{CaL} is increased and APD and QT intervals are prolonged, most likely because of reduced Ca^{2+}-induced Ca^{2+} release-dependent inactivation of this current. The degree of APD prolongation is exacerbated by inhibition of I_{Ks}. This contributes to increased BVR and

spatial dispersion of repolarization during ISO-induced diastolic Ca^{2+} release and, aside from DAD-mediated TA, may be an additional mechanism contributing to arrhythmogenesis. Pharmacological interventions that regularize SCR or inhibit SCR with or without preserved systolic contractions reduce BVR. Our data provide novel insights into arrhythmogenic mechanisms during increased Ca^{2+} loading.

Acknowledgments

The authors thank Drs Chris Pollard and Jean-Pierre Valentin, Department of Safety Pharmacology, Safety Assessment UK, AstraZeneca R&D, Alderley Park, United Kingdom, for active collaboration and for providing cardiac myocytes. Ongoing collaborations with Dr Yoram Rudy, Washington University, St. Louis, Missouri, and use of his computational resources are gratefully acknowledged.

Sources of Funding

P.G.A.V. is supported by a Vidi grant from the Netherlands Organization for Scientific Research (ZonMw 91710365). D.A. Eisner and A.W. Trafford are supported by the British Heart Foundation. D.M. Johnson was financially supported by AstraZeneca Ltd, United Kingdom.

Disclosures

None.

References

1. Bers DM. Cardiac excitation-contraction coupling. *Nature*. 2002;415:198–205.
2. Stern MD, Capogrossi MC, Lakatta EG. Spontaneous calcium release from the sarcoplasmic reticulum in myocardial cells: mechanisms and consequences. *Cell Calcium*. 1988;9:247–256.
3. Zygmunt AC, Goodrow RJ, Weigel CM. I_{NaCa} and $I_{Cl(Ca)}$ contribute to isoproterenol-induced delayed after depolarizations in midmyocardial cells. *Am J Physiol*. 1998;275:H1979–H1992.
4. Bers DM. Calcium cycling and signaling in cardiac myocytes. *Annu Rev Physiol*. 2008;70:23–49.
5. Volders PG, Kulcsar A, Vos MA, Sipido KR, Wellens HJ, Lazzara R, Szabo B. Similarities between early and delayed afterdepolarizations induced by isoproterenol in canine ventricular myocytes. *Cardiovasc Res*. 1997;34:348–359.
6. Ter Keurs HE, Boyden PA. Calcium and arrhythmogenesis. *Physiol Rev*. 2007;87:457–506.
7. Zaniboni M, Pollard AE, Yang L, Spitzer KW. Beat-to-beat repolarization variability in ventricular myocytes and its suppression by electrical coupling. *Am J Physiol Heart Circ Physiol*. 2000;278:H677–H687.
8. Hinterseer M, Beckmann BM, Thomsen MB, Pfeufer A, Ulbrich M, Sinner MF, Perz S, Wichmann HE, Lengyel C, Schimpf R, Maier SK, Varró A, Vos MA, Steinbeck G, Kääb S. Usefulness of short-term variability of QT intervals as a predictor for electrical remodeling and proarrhythmia in patients with nonischemic heart failure. *Am J Cardiol*. 2010;106:216–220.
9. Tereshchenko LG, Han L, Cheng A, Marine JE, Spragg DD, Sinha S, Dalal D, Calkins H, Tomaselli GF, Berger RD. Beat-to-beat three-dimensional ECG variability predicts ventricular arrhythmia in ICD recipients. *Heart Rhythm*. 2010;7:1606–1613.
10. Thomsen MB, Verduyn SC, Stengl M, Beekman JD, de Pater G, van Opstal J, Volders PG, Vos MA. Increased short-term variability of repolarization predicts d-sotalol-induced torsades de pointes in dogs. *Circulation*. 2004;110:2453–2459.
11. Gallacher DJ, Van de Water A, van der Linde H, Hermans AN, Lu HR, Towart R, Volders PG. In vivo mechanisms precipitating torsades de pointes in a canine model of drug-induced long-QT1 syndrome. *Cardiovasc Res*. 2007;76:247–256.
12. Jacobson I, Carlsson L, Duker G. Beat-by-beat QT interval variability, but not QT prolongation per se, predicts drug-induced torsades de pointes in the anaesthetised methoxamine-sensitized rabbit. *J Pharmacol Toxicol Methods*. 2011;63:40–46.
13. Hinterseer M, Beckmann BM, Thomsen MB, Pfeufer A, Dalla Pozza R, Loeff M, Netz H, Steinbeck G, Vos MA, Kääb S. Relation of increased short-term variability of QT interval to congenital long-QT syndrome. *Am J Cardiol*. 2009;103:1244–1248.
14. Johnson DM, Heijman J, Pollard CE, Valentin JP, Crijns HJ, Abi-Gerges N, Volders PG. I_{Ks} restricts excessive beat-to-beat variability of repolarization during beta-adrenergic receptor stimulation. *J Mol Cell Cardiol*. 2010;48:122–130.
15. Volders PG, Sipido KR, Vos MA, Spätjens RL, Leunissen JD, Carmeliet E, Wellens HJ. Downregulation of delayed rectifier K^+ currents in dogs with chronic complete atrioventricular block and acquired torsades de pointes. *Circulation*. 1999;100:2455–2461.
16. Dibb KM, Rueckschloss U, Eisner DA, Isenberg G, Trafford AW. Mechanisms underlying enhanced cardiac excitation contraction coupling observed in the senescent sheep myocardium. *J Mol Cell Cardiol*. 2004;37:1171–1181.
17. Heijman J, Volders PG, Westra RL, Rudy Y. Local control of ß-adrenergic stimulation: Effects on ventricular myocyte electrophysiology and Ca^{2+}-transient. *J Mol Cell Cardiol*. 2011;50:863–871.
18. Katra RP, Laurita KR. Cellular mechanism of calcium-mediated triggered activity in the heart. *Circ Res*. 2005;96:535–542.
19. Priori SG, Corr PB. Mechanisms underlying early and delayed afterdepolarizations induced by catecholamines. *Am J Physiol*. 1990;258:H1796–H1805.
20. Zhao Z, Wen H, Fefelova N, Allen C, Baba A, Matsuda T, Xie LH. Revisiting the ionic mechanisms of early afterdepolarizations in cardiomyocytes: predominant by Ca waves or Ca currents? *Am J Physiol Heart Circ Physiol*. 2012;302:H1636–H1644.
21. Overend CL, Eisner DA, O'Neill SC. The effect of tetracaine on spontaneous Ca^{2+} release and sarcoplasmic reticulum calcium content in rat ventricular myocytes. *J Physiol (Lond)*. 1997;502:471–479.
22. Venetucci LA, Trafford AW, Díaz ME, O'Neill SC, Eisner DA. Reducing ryanodine receptor open probability as a means to abolish spontaneous Ca^{2+} release and increase Ca^{2+} transient amplitude in adult ventricular myocytes. *Circ Res*. 2006;98:1299–1305.
23. Trafford AW, Sibbring GC, Díaz ME, Eisner DA. The effects of low concentrations of caffeine on spontaneous Ca release in isolated rat ventricular myocytes. *Cell Calcium*. 2000;28:269–276.
24. Anderson ME. Multiple downstream proarrhythmic targets for calmodulin kinase II: moving beyond an ion channel-centric focus. *Cardiovasc Res*. 2007;73:657–666.
25. Curran J, Hinton MJ, Ríos E, Bers DM, Shannon TR. Beta-adrenergic enhancement of sarcoplasmic reticulum calcium leak in cardiac myocytes is mediated by calcium/calmodulin-dependent protein kinase. *Circ Res*. 2007;100:391–398.
26. Kaseda S, Gilmour RF Jr, Zipes DP. Depressant effect of magnesium on early afterdepolarizations and triggered activity induced by cesium, quinidine, and 4-aminopyridine in canine cardiac Purkinje fibers. *Am Heart J*. 1989;118:458–466.
27. Aomine M, Tatsukawa Y, Yamato T, Yamasaki S. Antiarrhythmic effects of magnesium on rat papillary muscle and guinea pig ventricular myocytes. *Gen Pharmacol*. 1999;32:107–114.
28. Watanabe H, Chopra N, Laver D, Hwang HS, Davies SS, Roach DE, Duff HJ, Roden DM, Wilde AA, Knollmann BC. Flecainide prevents catecholaminergic polymorphic ventricular tachycardia in mice and humans. *Nat Med*. 2009;15:380–383.
29. Trafford AW, Díaz ME, Eisner DA. Ca-activated chloride current and Na-Ca exchange have different timecourses during sarcoplasmic reticulum Ca release in ferret ventricular myocytes. *Pflugers Arch*. 1998;435:743–745.
30. Myles RC, Wang L, Kang C, Bers DM, Ripplinger CM. Local ß-adrenergic stimulation overcomes source-sink mismatch to generate focal arrhythmia. *Circ Res*. 2012;110:1454–1464.
31. Trafford AW, Díaz ME, Negretti N, Eisner DA. Enhanced Ca^{2+} current and decreased Ca^{2+} efflux restore sarcoplasmic reticulum Ca^{2+} content after depletion. *Circ Res*. 1997;81:477–484.
32. Takamatsu H, Nagao T, Ichijo H, Adachi-Akahane S. L-type Ca^{2+} channels serve as a sensor of the SR Ca^{2+} for tuning the efficacy of Ca^{2+}-induced Ca^{2+} release in rat ventricular myocytes. *J Physiol (Lond)*. 2003;552:415–424.
33. Spencer CI, Sham JS. Effects of Na^+/Ca^{2+} exchange induced by SR Ca^{2+} release on action potentials and afterdepolarizations in guinea pig ventricular myocytes. *Am J Physiol Heart Circ Physiol*. 2003;285:H2552–H2562.

34. Burashnikov A, Antzelevitch C. Block of I_{Ks} does not induce early afterdepolarization activity but promotes β-adrenergic agonist-induced delayed afterdepolarization activity. *J Cardiovasc Electrophysiol*. 2000;11:458–465.
35. Lerche C, Seebohm G, Wagner CI, Scherer CR, Dehmelt L, Abitbol I, Gerlach U, Brendel J, Attali B, Busch AE. Molecular impact of MinK on the enantiospecific block of I_{Ks} by chromanols. *Br J Pharmacol*. 2000;131:1503–1506.
36. Bárándi L, Virág L, Jost N, Horváth Z, Koncz I, Papp R, Harmati G, Horváth B, Szentandrássy N, Bányász T, Magyar J, Zaza A, Varró A, Nánási PP. Reverse rate-dependent changes are determined by baseline action potential duration in mammalian and human ventricular preparations. *Basic Res Cardiol*. 2010;105:315–323.
37. Sipido KR, Volders PG, de Groot SH, Verdonck F, Van de Werf F, Wellens HJ, Vos MA. Enhanced Ca^{2+} release and Na/Ca exchange activity in hypertrophied canine ventricular myocytes: potential link between contractile adaptation and arrhythmogenesis. *Circulation*. 2000;102:2137–2144.
38. Morotti S, Grandi E, Summa A, Ginsburg KS, Bers DM. Theoretical study of L-type Ca^{2+} current inactivation kinetics during action potential repolarization and early afterdepolarizations. *J Physiol (Lond)*. 2012;590:4465–4481.
39. Hashambhoy YL, Winslow RL, Greenstein JL. CaMKII-induced shift in modal gating explains L-type Ca^{2+} current facilitation: a modeling study. *Biophys J*. 2009;96:1770–1785.

Novelty and Significance

What Is Known?

- Beat-to-beat variability of ventricular repolarization (BVR) duration has been proposed as a more predictive marker of Torsades de Pointes (TdP) arrhythmia than repolarization duration alone. The cellular mechanisms of BVR remain to be fully elucidated.
- During intense β-adrenergic receptor stimulation, Ca^{2+} load of the myocyte increases. Additional blockade of the slowly activating delayed-rectifier K^+ current (I_{Ks}) amplifies this effect and exaggerates BVR.
- Spontaneous sarcoplasmic reticulum Ca^{2+} release (SCR) during Ca^{2+} overload can cause membrane depolarization via Ca^{2+}-dependent ion currents, resulting in afterdepolarizations and, potentially, triggered activity.

What New Information Does This Article Contribute?

- In canine left ventricular myocytes, late diastolic SCR during β-adrenergic stimulation causes prolongation of the following action potential (AP), especially during I_{Ks} blockade. The irregular occurrence of SCR exaggerates BVR by interspersed AP prolongation. Pharmacological interventions that prevent or regularize SCR reduce BVR.
- By sarcoplasmic reticulum unloading, late diastolic SCR decreases systolic sarcoplasmic reticulum Ca^{2+} release during the following AP. This reduces Ca^{2+}-dependent inactivation of the L-type Ca^{2+} current, causing the AP prolongation.
- In a canine model of drug-induced long-QT1 syndrome, β-adrenergic challenges cause paradoxical repolarization prolongation, exaggerated BVR, and aftercontractions just before the initiation of TdP. QT, monophasic AP, and T_{peak}-T_{end} interval of the beats after aftercontractions are significantly prolonged. The Ca^{2+} antagonist verapamil prevents aftercontractions and arrhythmia.

A significant increase in BVR has been observed in animal models and selected human subjects before TdP onset. The in vivo mechanisms of this remain incompletely understood but reside partly in the cardiac myocyte. Cellular Ca^{2+} overload can augment BVR and plays a major role in arrhythmogenesis. Here, we aimed at elucidating Ca^{2+}-dependent mechanisms of augmented BVR during β-adrenergic stimulation and I_{Ks} blockade, in effect mimicking long-QT1 syndrome. We show that APs prolong significantly after SCR, leading to increased BVR if the occurrence of SCR is irregular. An intact I_{Ks} prevents much of the repolarization prolongation. AP prolongation is driven by reduced Ca^{2+}-dependent inactivation of L-type Ca^{2+} current resulting from decreased systolic sarcoplasmic reticulum Ca^{2+} release after SCR. Pharmacological interventions that prevent or regularize SCR reduce BVR, which suggests novel antiarrhythmic approaches against TdP under these conditions. We also demonstrate that during β-adrenergic stimulation and I_{Ks} blockade in vivo, paradoxical prolongation of repolarization and aftercontractions precede TdP, suggesting that the identified cellular mechanisms have relevance for arrhythmogenesis in the intact heart. Thus, myocardial Ca^{2+} overload and delayed and early afterdepolarizations not only can cause arrhythmias via triggered activity but also by increasing temporal and spatial dispersion of repolarization, promoting reentrant excitation.

Circulation Research
JOURNAL OF THE AMERICAN HEART ASSOCIATION

Diastolic Spontaneous Calcium Release From the Sarcoplasmic Reticulum Increases Beat-to-Beat Variability of Repolarization in Canine Ventricular Myocytes After β-Adrenergic Stimulation

Daniel M. Johnson, Jordi Heijman, Elizabeth F. Bode, David J. Greensmith, Henk van der Linde, Najah Abi-Gerges, David A. Eisner, Andrew W. Trafford and Paul G.A. Volders

Circ Res. 2013;112:246-256; originally published online November 13, 2012;
doi: 10.1161/CIRCRESAHA.112.275735
Circulation Research is published by the American Heart Association, 7272 Greenville Avenue, Dallas, TX 75231

Print ISSN: 0009-7330. Online ISSN: 1524-4571

Diastolic Spontaneous Calcium Release from the Sarcoplasmic Reticulum Increases Beat-to-Beat Variability of Repolarization in Canine Ventricular Myocytes after β-Adrenergic Stimulation

Supplemental Material

Daniel M. Johnson,[*] Jordi Heijman[*], Elizabeth F. Bode, David J. Greensmith, Henk van der Linde, Najah Abi-Gerges, David A. Eisner, Andrew W. Trafford, Paul G.A. Volders

* These authors contributed equally to this work

Corresponding Author:
Paul G.A. Volders, MD, PhD
Department of Cardiology
Cardiovascular Research Institute Maastricht
Maastricht University Medical Centre
P.O. Box 5800
6202 AZ Maastricht
The Netherlands
e-mail: p.volders@maastrichtuniversity.nl
phone: +31 43 3875094
fax: +31 43 3875104

Extended Methods

Cell-isolation procedure

Adult female beagle dogs were used for the myocyte isolations. Anesthesia was induced with 45 mg/kg pentobarbital. Once full anesthesia was reached, the chest was opened via a left thoracotomy and the heart was excised and placed in an O_2-gassed Ca^{2+}-free standard buffer solution at approximately 4 °C. The cell-isolation procedure was the same as previously described.[1] Briefly the left-anterior descending coronary artery was cannulated and perfused. After ~20 min of collagenase perfusion and subsequent washout of the enzyme, the epicardial surface layer was removed from the LV wedge until a depth of ≥3 mm was reached. Softened tissue samples were collected from the midmyocardial layer underneath while contamination with the epi- and endocardium was avoided. Samples were gently agitated, filtered and washed. LV midmyocytes were stored at room temperature in standard buffer solution (vide infra) and only quiescent rod-shaped cells with clear cross-striations were used for the experiments. Cells were used within 48 h of isolation.

Sharp-electrode action potential recordings

Transmembrane action potentials (APs) were recorded at 37 °C using high-resistance (30–60 MΩ) glass microelectrodes filled with 3 mol/L KCl with a microelectrode amplifier (Axoclamp-2B, Axon Instruments, Inc). Intracellular pacing was done at various cycle lengths (CLs; 500 ms – 2000 ms). Only cells showing a stable spike-and-dome AP morphology and resting membrane potential were accepted for the experiments. Myocyte contractions were recorded with a video edge motion detector (Crescent Electronics, Sandy, UT, USA).

Ca^{2+} measurements

Isolated myocytes were loaded with the acetoxymethyl ester of indicator Fluo-3 or Fura-2 (Molecular Probes; 5 µmol/L, 5 min loading and 30 min de-esterification). Electrophysiological control for current-clamp and voltage-clamp experiments with simultaneous $[Ca^{2+}]_i$ measurements was achieved using the perforated patch clamp technique with amphotericin-B (240 µg/ml). The switch-clamp facility (frequency 1–3 kHz and gain 1–3) of the Axoclamp-2B voltage clamp amplifier (Axon Instruments, CA, USA) was used to overcome the access resistance of the perforated patch. All experiments were performed at 37 °C.

Drugs and experimental solutions

The standard buffer solution used for the experiments was composed of (in mmol/L): NaCl 145, KCl 4.0, $CaCl_2$ 1.8, $MgCl_2$ 1.0, glucose 11 and HEPES 10, pH 7.4 with NaOH at 37 °C. In a subset of experiments, extracellular [Mg^{2+}] was increased to 5 mmol/L by the addition of 4 mmol/L $MgSO_4$. In other experiments, extracellular [Ca^{2+}] was increased to 3.6 mmol/L to further increase cellular Ca^{2+} loading.

500 nmol/L HMR1556 ((3R,4S)-(+)-N-[3-hydroxy-2,2-dimethyl-6-(4,4,4-trifluorobutoxy)chroman-4-yl]-N-methylmethanesulfonamide; a gift from Dr. H. Gögelein, Sanofi-Aventis Germany GmbH, Frankfurt, Germany) was used to selectively and completely block I_{Ks}.[2-4] Sarcoplasmic reticulum (SR) Ca^{2+} release through the ryanodine receptor (RyR) was inhibited with 1 µmol/L ryanodine (RBI, Natick, MA, USA) or stabilized using 5 µmol/L tetracaine (Sigma-Aldrich Zwijndrecht, The Netherlands). Caffeine (Sigma-Aldrich Zwijndrecht, The Netherlands; maximally 500 µmol/L) was used to increase RyR open probability. Ca^{2+}/Calmodulin-dependent kinase (CaMKII) activity was modulated using the CaMKII inhibitor KN93 (Sigma-Aldrich Zwijndrecht, The Netherlands; 5 µmol/L) and the calmodulin inhibitor W7 (Tocris Bioscience, Bristol, UK; 1 µmol/L). The class-1C antiarrhythmic agent flecainide (MedaPharma, Amstelveen, The Netherlands) was employed in a subset of experiments. At 6 µmol/L, flecainide results in a 40% decrease in RyR activity[5] as well as affecting multiple other targets (40% inhibition of I_{To}[6], significant inhibition of (late) I_{Na}[7] and ~50% inhibition of HERG K^+ channels[8]).

For perforated patch experiments the patch pipette solution contained (in mmol/L): KCH_3O_3S 125, KCl 20, NaCl 10, HEPES 10, $MgCl_2$ 5, K_2EGTA 0.1, titrated to 7.2 with KOH with patch pipette resistance being 2-3 MΩ. In voltage clamp experiments, K^+ currents were blocked by addition of 500 nmol/L HMR1556, 5 mmol/L 4-aminopyridine and 100 nmol/L $BaCl_2$ to the standard buffer solution. Extracellular Ca^{2+} was raised (to 3.6 or 5.0 mmol/L) to further enhance cellular Ca^{2+} loading.

HMR1556, ryanodine, tetracaine, caffeine, W7 and KN93 were initially dissolved in dimethyl sulfoxide (DMSO) and then diluted so that the concentration of the solvent was maximally 0.1% in the superfusate, a concentration that has no measurable effects on AP or ionic currents.

βAS was applied by 100 nmol/L isoproterenol in all experiments. This agent was originally dissolved in distilled water containing 30 µmol/L ascorbic acid and then stored in the dark at 4 °C until use.

When assessing the effect of pharmacological interventions, all conditions were kept constant for several minutes until APD and cell shortening reached steady state. Analyses were performed using these steady-state data.

Data analysis

Detection of EADs, DADs and determination of APD, BVR and DAD parameters was done in a semi-automated fashion using a custom Matlab (The Mathworks, Natick, MA, USA) script. Briefly, Axon (Axon Instruments, CA, USA) data files were loaded into Matlab. AP upstroke was detected based on peaks in the numerically calculated dV/dt, and APD_{90} was determined. Subsequently, the diastolic interval between APD_{90} of one beat and the point of maximum dV/dt of the next beat was processed for all beats. The signal was low-pass filtered at 30 Hz to reduce noise. All peaks in the filtered signal were determined and resting membrane potential was defined as the average value between the smallest (most negative) local maximum and local minimum. The amplitude of all other peaks was determined relative to this resting membrane potential. DADs were identified as a local maximum in the filtered signal of more than 2 mV in amplitude and manually confirmed by the investigators. EADs were detected as positive local maxima in the low-pass filtered dV/dt signal preceded and followed by negative local minima. Detection of EADs was manually validated.

BVR was determined using a sliding window of 30 consecutive beats using: $\Sigma(|APD_{i+1} - APD_i|)/[n_{beats} \times \sqrt{2}]$, and mean BVR for a given condition (CL and/or pharmacological intervention) was determined for each cell.

In-vivo dog model of LQT1

TdP arrhythmias were induced in an in-vivo dog model of long-QT1 syndrome as previously described.[9] Briefly, general anesthesia was induced in 10 beagle dogs by lofentanil (0.075 mg/kg body weight i.v.), scopolamine (0.015 mg/kg), succinylcholine (1.0 mg/kg), hourly slow injections of fentanyl (0.025 mg/kg i.v.), and continuous infusion of etomidate (1.5 mg/kg/hour). Dogs were ventilated with 30% oxygen in pressurized air to normocapnia. The body temperature was kept at 37 °C with a heated water mattress. ECG standard lead II was

continuously recorded and the QT interval (QT; ms) measured from the onset of the QRS to the final end of the T wave. Left ventricular (LV) intracavitary pressures were recorded with high-fidelity catheter-tip micromanometers (Gaeltec Ltd, Dunvegan, UK and Millar Instruments Inc, Houston, TX). Under fluoroscopic guidance a MAP catheter (Boston Scientific-EP Technologies, San Jose, CA) was placed at the endocardium of the LV and RV, near the apical septum.

HMR1556 (dissolved in 20% HP-β-cyclodextrin) was infused i.v. in the dogs, initially at a rate of 0.025 mg/kg/min for 30 min and followed (if necessary) by infusions at 0.05 mg/kg/min and 0.1 mg/kg/min. At regular time intervals, boluses of isoproterenol (1.25, 2.5 or 5 μg/kg) were injected to induce torsades de pointes and in prevention experiments verapamil (0.4 mg/kg) was infused pre-isoproterenol challenge after confirming TdP inducibility with HMR1556 + ISO in the same animal. External electrical cardioversion was applied to terminate sustained TdP or its deterioration into ventricular fibrillation, if induced by isoproterenol.

Computational modeling

A recent model of the canine ventricular myocyte electrophysiology including βAR stimulation[10] was extended to induce diastolic SR Ca^{2+} release in a controlled fashion, similar to a recent approach by Xie et al.[11] Both timing (start, duration) and amplitude of diastolic SR Ca^{2+} release could be controlled.

In particular, the model was divided into two identical domains (**Online Figure I**) coupled by Ca^{2+} diffusion between cytosol and network SR to simulate the local origin of SCR. Diffusion time constants were based on the local control model by Restrepo et al.[12] and diffusion was significantly slower in SR compared to cytosol, consistent with experimental observations[13]. The late component of I_{Na} (I_{NaL}) was increased in the model to simulate the midmyocardial origin of the myocytes used in our experiments, consistent with experimental data from Zygmunt et al.[14] Model APD rate dependence at baseline, in the presence of ISO and in the presence of ISO+HMR1556 (simulated as 100% inhibition of I_{Ks}) was consistent with experimental data (**Online Figure IIA**). Parameters of the L-type Ca^{2+} current (I_{CaL}) were adjusted based on the experiments in the presence of ryanodine to obtain quantitative agreement on the amount of APD prolongation in the absence of SR Ca^{2+} release.

To initiate SCR, steady-state RyR activation was set to a constant value in one of the two domains for the interval of diastolic SR Ca^{2+} release such that the desired reduction in local JSR

Ca^{2+} was achieved. When steady-state RyR activation was set to 0.375 ($SCR_{level} = 0.375$) from t = 925 ms until t = 950 ms (at CL = 1000 ms), the SCR-induced prolongation of APD was consistent with experimental observations (**Online Figure IIB**).

The model was paced to steady state (2000 seconds of pacing) in the presence of βAR stimulation with or without I_{Ks} inhibition, to mimic experimental conditions. The effect of diastolic SR Ca^{2+} release was examined by determining APD of a single beat at steady-state as a function of the timing and amplitude of the preceding diastolic Ca^{2+} release. In some simulations other currents / fluxes (I_{CaL}, I_{NaCa}, $I_{Cl(Ca)}$, J_{rel}) were blocked for the duration of this final beat.

One-dimensional strand simulations were performed as previously described.[15] Steady-state conditions of single-cell simulations in the presence of ISO and I_{Ks} blockade were used as initial conditions for the homogeneous strand of 128 cells. The strand was subsequently paced by direct stimulation of the first 3 cells (-80 pA/pF for 2.0 ms) for 100 seconds to achieve steady-state conditions for the strand. The effect of diastolic SR Ca^{2+} release was determined by applying the methodology described above to *k* cells in the middle of the strand. SR Ca^{2+} release was initiated simultaneously in all *k* cells. The exact mechanisms by which SCR synchronizes across a sufficient number of myocytes to generate ventricular ectopic beats remain incompletely understood. Recent research by Wasserstrom et al. has suggested that an intrinsic synchronization occurs due to a decrease in variability of SCR events with increasing Ca^{2+} load.[16, 17] Furthermore, Myles et al. have shown that localized βAR can produce spatiotemporal synchronization of SR Ca^{2+} overload and release, which can produce focal activity and arrhythmia in normal rabbit hearts.[18] Although direct diffusion of Ca^{2+} between cells through gap junctions could further contribute to the synchronization of SCR,[19] this was not implemented in the current model because the main goal of the present research was to determine the electrophysiological consequences of SCR, independent of the synchronization method.

A similar approach was used to study the effect of diastolic SR Ca^{2+} release on homogeneous two-dimensional sheets of virtual 'tissue'. The tissue size was 2 x 2 cm and was simulated using 200 x 200 grid points, in line with previous studies.[20, 21] Steady-state conditions of single-cell simulations in the presence of ISO and I_{Ks} blockade were used as initial conditions and 5 beats were simulated following stimulation of the left-most column of 200 cells (-80 pA/pF for 2.0 ms),

resulting in a planar wave activating the entire sheet. Conduction velocity was 49 cm/s. Diastolic SR Ca^{2+} release was initiated simultaneously in 25% of the 40.000 cells surrounding the center of the tisues (i.e., cells with x and y coordinates between 50 and 150).

Alterations in model equations compared to Heijman et al.[10]:

The superscript symbol x, is used to designate one of the two identical Ca^{2+} domains. Whole-cell concentrations / currents are defined as the average of both domains and are indicated without superscript x.

Altered I_{NaL}:

$$I_{NaL}^{NP} = 1.6 \cdot 6.500 \cdot 10^{-3} \cdot (m_L)^3 \cdot h_L \cdot (V_m - E_{Na})$$

$$I_{NaL}^{P,CaMK} = 1.6 \cdot 1.600 \cdot 10^{-2} \cdot (m_L)^3 \cdot h_L \cdot (V_m - E_{Na})$$

Altered I_{CaL}:

$$I_{V,\tau}^{P} = \frac{1}{\frac{1}{70.0 \cdot \left(1 + \exp\left((V_m + 49.10)/10.349\right)\right)} + \frac{1}{75 \cdot \left(1 + \exp(-(V_m + 0.213)/10.807)\right)}}$$

$$I_{V,\infty}^{P} = \frac{1}{1.02} \cdot \left(0.02 + \frac{1}{1 + \exp\left((V_m + 29.979)/3.1775\right)}\right)$$

$$Is_{V,\infty}^{P} = \frac{1}{1.0004} \cdot \left(0.0004 + \frac{1}{1 + \exp\left((V_m + 29.979)/3.1775\right)}\right)$$

Altered RyR:

$$h_R = 10$$

$$I_{Rel,\infty}^{NP} = \frac{\alpha_{Rel}}{1 + \left(\frac{K_{Rel,\infty}}{[Ca^{2+}]_{JSR}^{x}}\right)^{h_R}} \cdot \frac{I_{ICaL}^{x}}{1 + \exp\left(\frac{(I_{ICaL}^{x} + 1.5)}{0.0001}\right)} - SCR_{level}$$

$$I_{Rel,\infty}^{P} = 1.9925 \cdot \frac{\alpha_{Rel}}{1 + \left(\frac{K_{Rel,\infty}}{[Ca^{2+}]_{JSR}^{x}}\right)^{h_R}} \cdot \frac{I_{ICaL}^{x}}{1 + \exp\left(\frac{(I_{ICaL}^{x} + 1.5)}{0.0001}\right)} - SCR_{level}$$

Altered Ca^{2+} diffusion:

$$I_{tr}^{x} = \frac{[Ca^{2+}]_{NSR}^{x} - [Ca^{2+}]_{JSR}^{x}}{\tau_{tr}}, \qquad \tau_{tr} = 100\ ms$$

$$I_{Diff,cyt}^{x} = \frac{[Ca^{2+}]_{i}^{y} - [Ca^{2+}]_{i}^{x}}{\tau_{Diff,cyt}}, \qquad \tau_{Diff,cyt} = 1.00\ ms, \qquad y: \text{other } Ca^{2+} \text{ domain}$$

$$I_{Diff,nsr}^{x} = \frac{[Ca^{2+}]_{NSR}^{y} - [Ca^{2+}]_{NSR}^{x}}{\tau_{Diff,nsr}}, \qquad \tau_{Diff,nsr} = 25.0\ ms, \qquad y: \text{other } Ca^{2+} \text{ domain}$$

$$\frac{d[Ca^{2+}]_{i,t}^{x}}{dt} = -\left(\frac{\left(I_{Ca,b}^{x} + I_{pCa}^{x} - 2 \cdot I_{NaCa,i}^{x}\right) \cdot C_{sc} \cdot A_{cap}}{z_{Ca} \cdot F \cdot V_{myo}} + I_{up}^{x} \cdot \frac{V_{nsr}}{V_{myo}} - I_{Diff}^{x} \cdot \frac{V_{SS,SR}}{V_{myo}} - I_{Diff,cyt}^{x}\right)$$

$$\frac{d[Ca^{2+}]_{NSR}^{x}}{dt} = I_{up}^{x} - I_{tr}^{x} \cdot \frac{V_{JSR}}{V_{NSR}} + I_{Diff,nsr}^{x}$$

Supplemental Figures

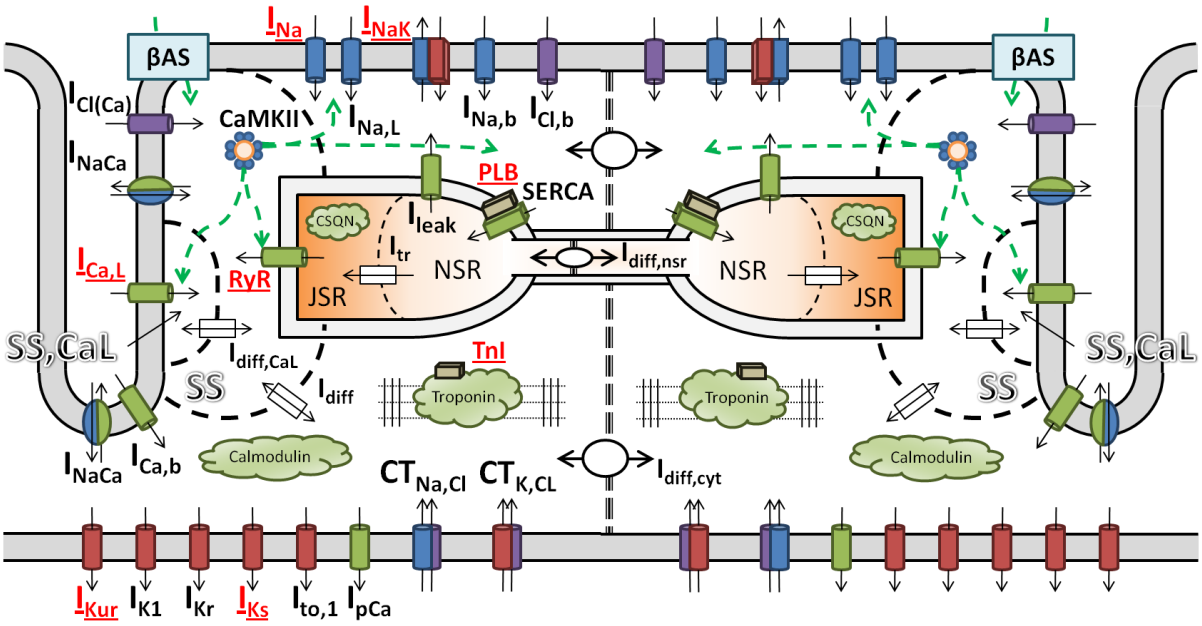

Online Figure I. Schematic overview of the computational model of the canine ventricular myocyte. Adapted from Heijman et al.[10] The model was divided into two identical domains to simulate the local origin of SCR. Only components on the left side of the model are labeled for clarity, identical components are located on the right side. The domains are coupled via diffusion of Ca^{2+} ($I_{diff,cyt}$ and $I_{diff,nsr}$). All other abbreviations are as previously described.[10]

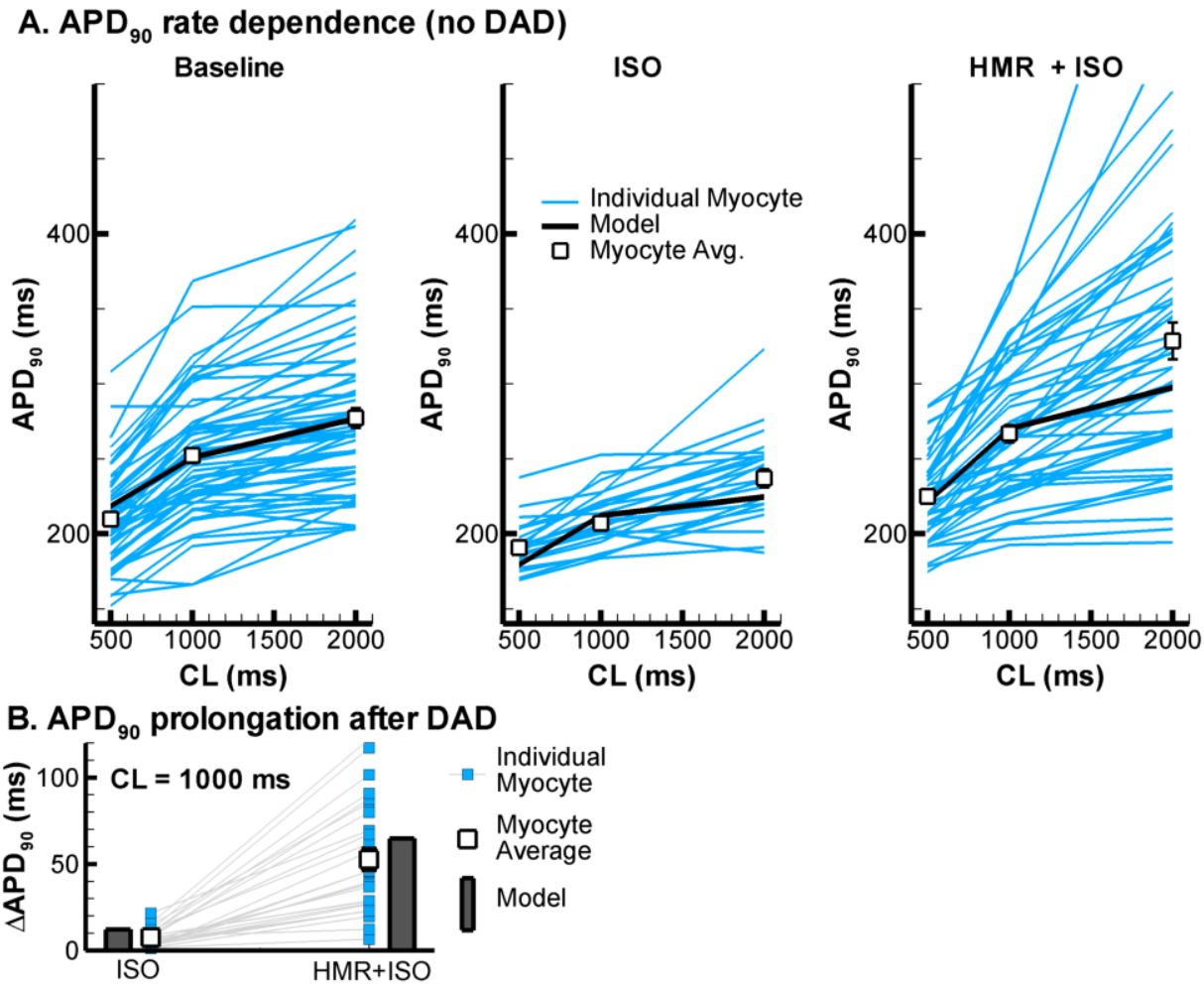

Online Figure II. Validation of model properties. **A.** Steady-state APD-rate dependence under baseline conditions (left panel), in the presence of ISO (middle panel) or in the presence of ISO + HMR1556 (right panel) for APs without prior DAD. Average APD for each cell is shown in blue. Average APD over all myocytes is indicated with symbols. Model APD is shown in black. Model APD-rate dependence falls within experimental range and is close to the experimental average for all conditions and CLs. **B.** Average APD difference between APs preceded by a DAD and those without prior DAD in the presence of ISO or ISO + HMR1556. Average APD difference for each cell is shown in blue. Average group data is indicated with symbols. Model APD prolongation after SCR is indicated with grey bars. Model APD prolongation is consistent with experimental observations.

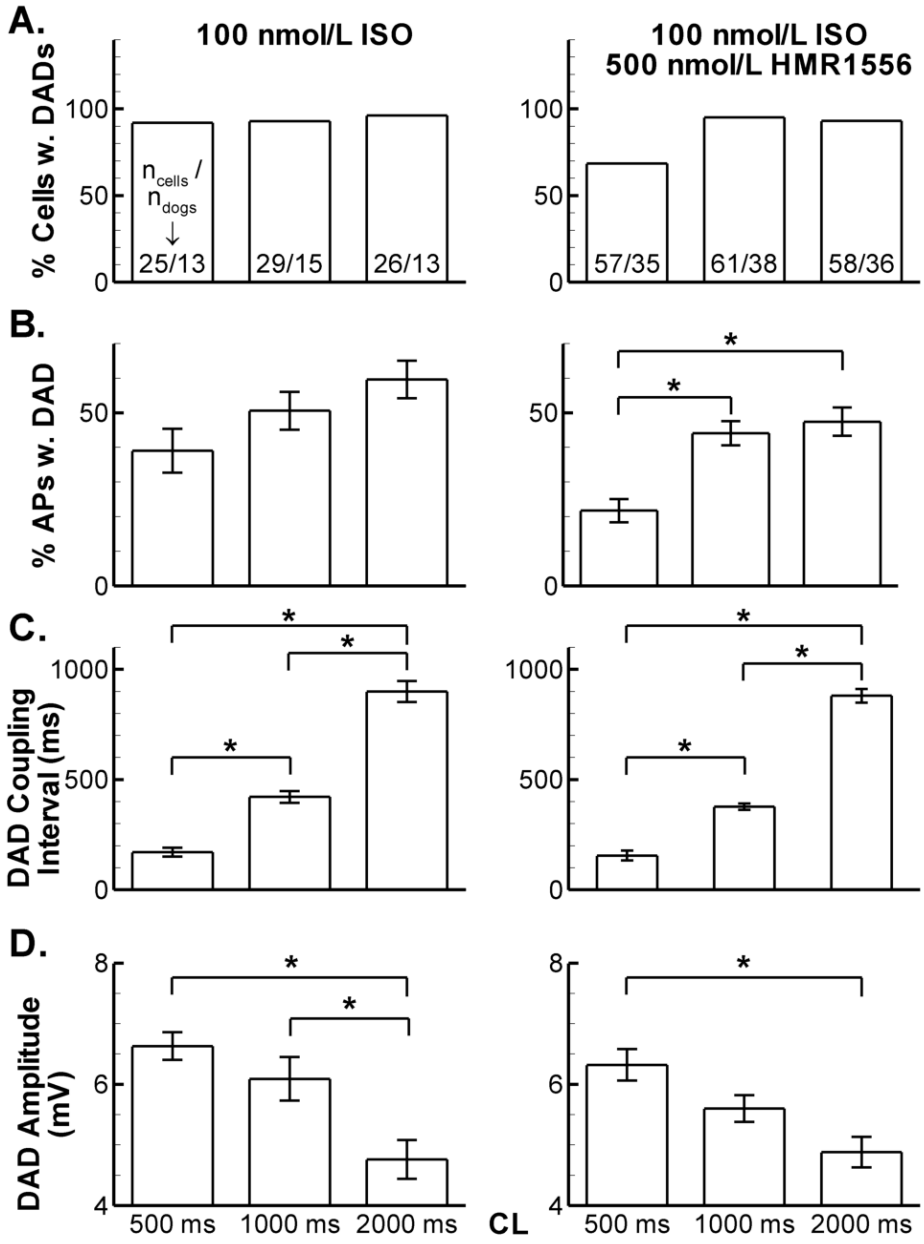

Online Figure III. Rate-dependent characteristics of DADs in the presence of ISO (left panels) or ISO + HMR1556 (right panels). **A.** Percentage of cells which showed DADs during βARS. Number of cells and number of dogs are indicated in each bar. **B.** Average percentage of APs which had a DAD. **C.** Coupling interval between end of repolarization (APD_{90}) and subsequent DAD for those beats which showed a DAD. **D.** Average DAD amplitude. * indicates $P<0.05$ based on one-way ANOVA with Tukey-Kramer post-hoc test. DADs occur earlier and are larger at faster rates. Data are consistent with those of Prior and Corr[22] in canine ventricular myocytes measured using a pace-pause protocol.

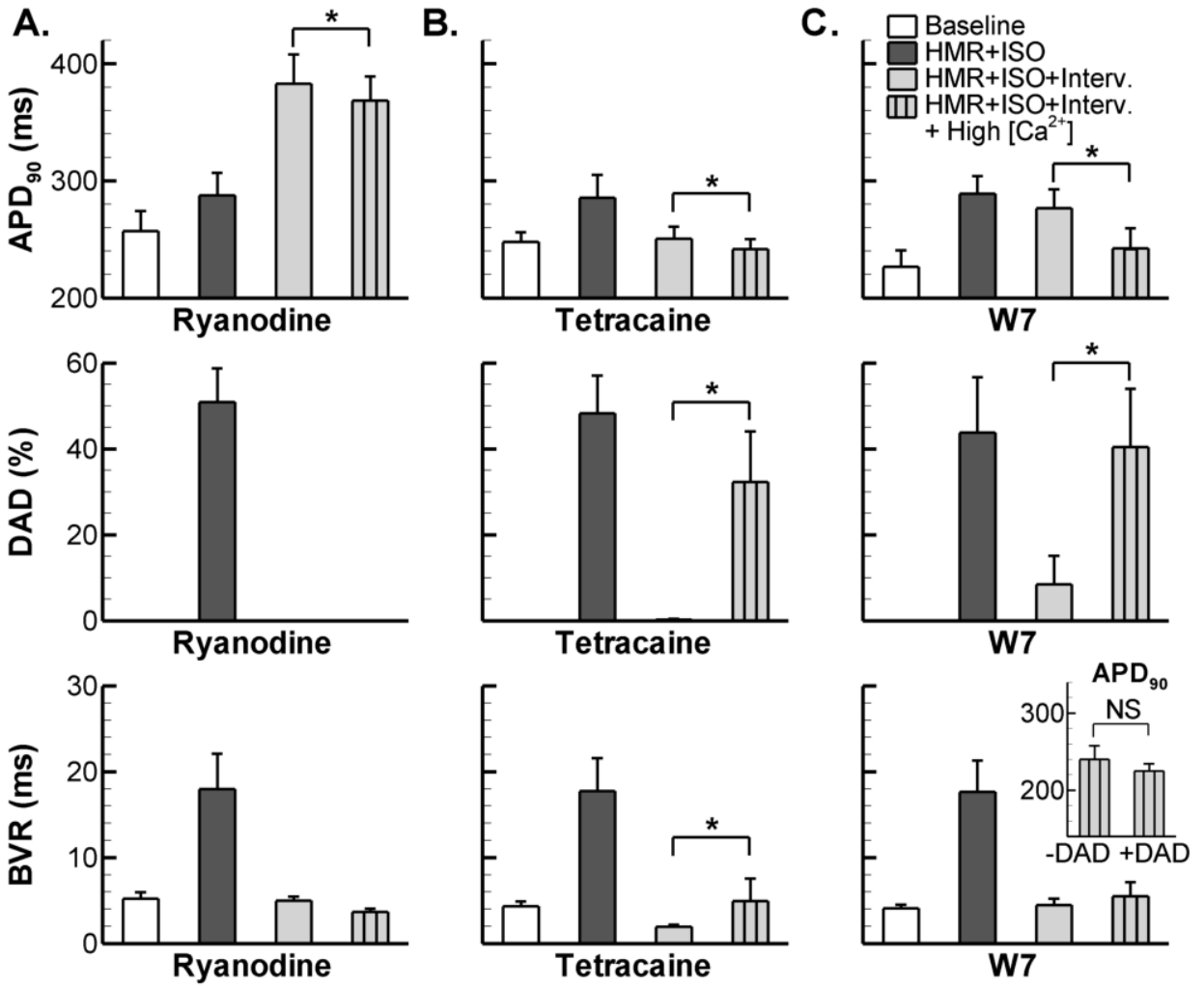

Online Figure IV. Effect of increased $[Ca^{2+}]_o$ on APD_{90} (top panels), DAD occurrence (middle panels), and BVR (bottom panels) under baseline conditions, HMR1556 + ISO, HMR1556 + ISO + Intervention or HMR1556 + ISO + Intervention + 3.6 mmol/L $[Ca^{2+}]_o$. **A**. Ryanodine. **B**. Tetracaine. **C**. W7. * indicates $P<0.05$. Only significance of intervention versus intervention in the presence of high $[Ca^{2+}]_o$ is indicated for clarity reasons. Inset in lower-right panel shows APD_{90} in the presence of HMR1556 + ISO + W7 + increased $[Ca^{2+}]_o$ for beats in the absence or presence of a preceding DAD.

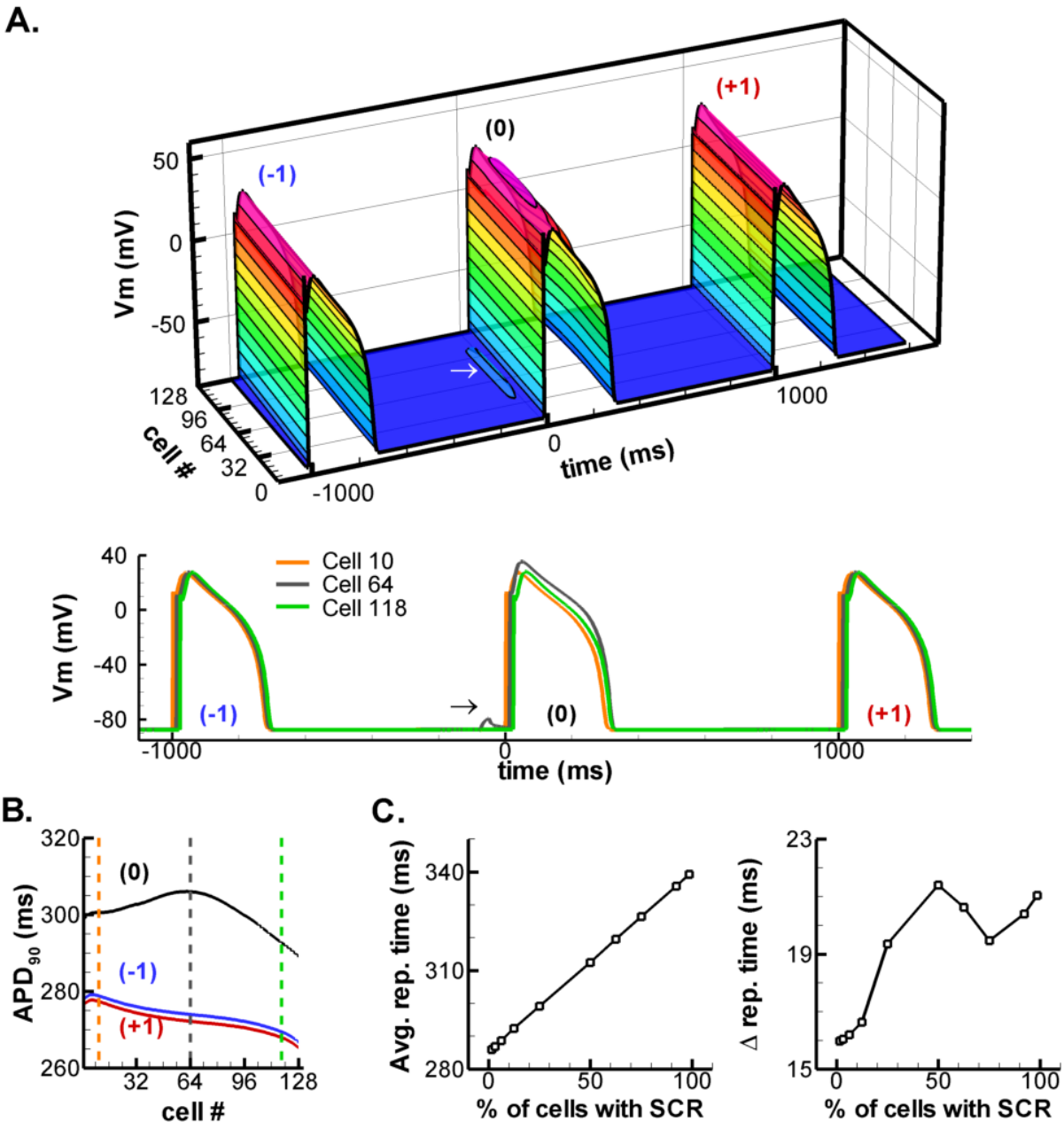

Online Figure V. Multicellular simulations in a one-dimensional strand of 128 cells in the presence of ISO and I_{Ks} blockade. **A.** APs during steady-state pacing at CL = 1000 ms (top panel). Prior to beat (0), diastolic SR Ca^{2+} release was initiated in cells 32-96 (arrow). The bottom panel shows an overlay of Vm for cell 10 (orange, no DAD), cell 64 (grey, with DAD indicated by arrow) and cell 118 (green, no DAD) for these three beats. **B.** APD_{90} for all cells in the strand for these 3 beats. Cells 10, 64 and 118 have been indicated by vertical dashed lines. The presence of a preceding 'spontaneous' diastolic SR Ca^{2+} release (SCR) causes a pronounced prolongation of APD_{90} of beat (0) throughout the strand (black line). In addition, an

increase in the spatial dispersion of repolarization could be observed. **C.** Average repolarization time (activation time + APD_{90}; left panel) and spatial dispersion of repolarization (maximum repolarization time – minimum repolarization time; right panel) as a function of the number of cells with SCR. SCR caused a progressive increase in the average repolarization time. Dispersion of repolarization was influenced by the number of cells with SCR (with a maximum around 50%). A low spatial dispersion of repolarization was expected at 100%, when all cells exhibit SCR. However, spatial dispersion of repolarization also depends on the timing of the SCR. Since SCR was initiated at the same time in all cells, but the time of Ca^{2+}-induced Ca^{2+}-release differs due to AP propagation along the strand, there is a longer time for SR refilling after the SCR in cell 128 than in cell 1. As such, the amount of APD prolongation differs throughout the strand resulting in an increased spatial dispersion even at 100%. Spatial dispersion of repolarization is a complex, non-monotonic function that depends on the number of cells with SCR, their location in the strand, the timing of the SCR and the conduction velocity.

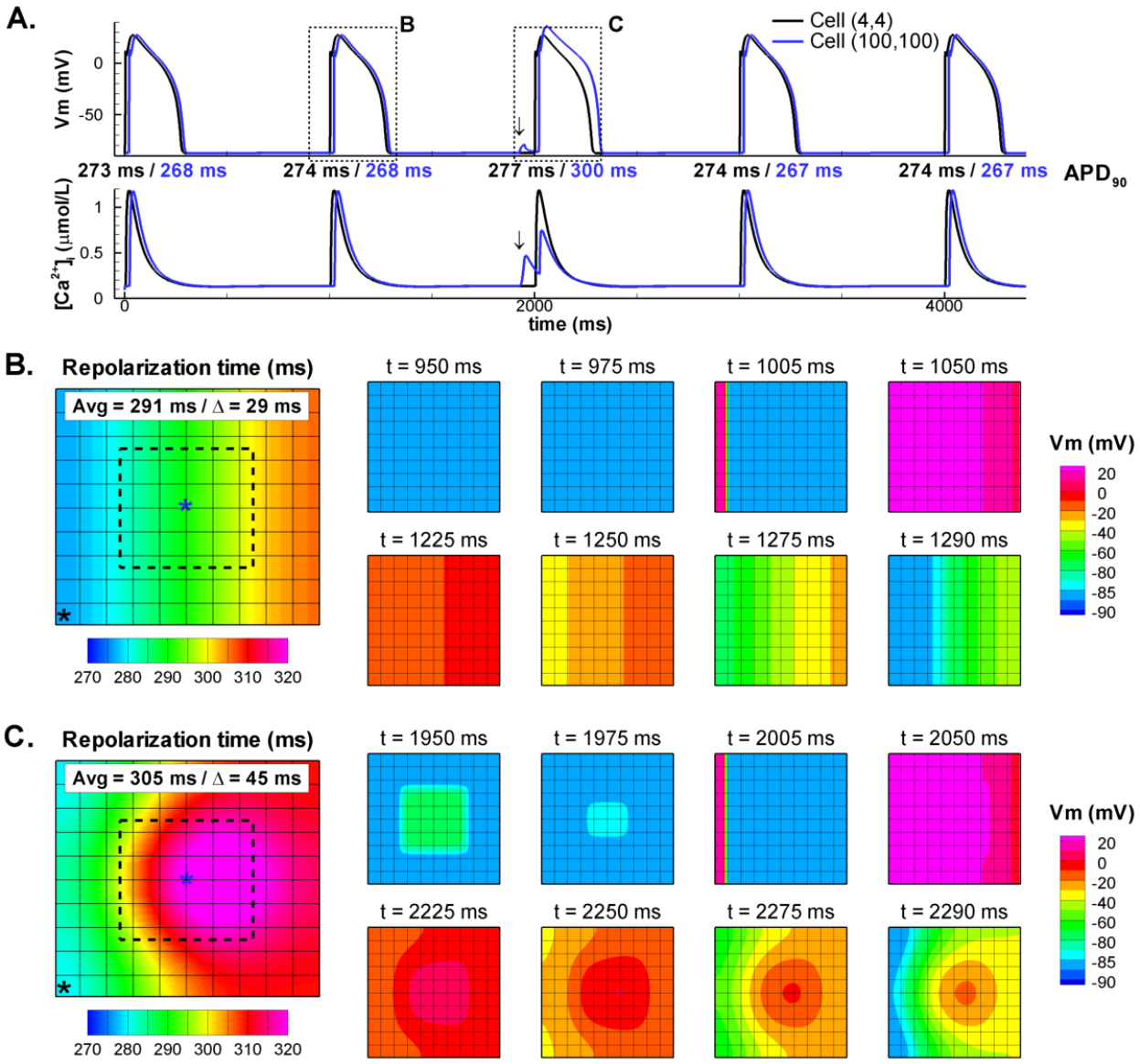

Online Figure VI. Multicellular simulations in homogeneous two-dimensional tissue of 200x200 nodes in the presence of ISO and I_{Ks} blockade. **A.** APs (top panel) and $[Ca^{2+}]_i$ (bottom panel) for 5 beats during steady-state pacing at 1000-ms CL for a cell on the edge of the tissue (at coordinates (4,4), black lines) and a cell in the center of the tissue (blue lines). The location of these cells is indicated with stars in panels B and C (left). APD_{90} of each AP is given below each beat in the corresponding color. Diastolic SR Ca^{2+} release was induced from 1925 to 1950 ms (indicated by arrows) for a region of 100x100 cells (25% of the cells) around the center of the tissue (i.e., cells with x and y coordinates between 50 and 150, dashed box in panels B and C). **B.** Spatial electrophysiological properties of beat 2. The left panel shows repolarization time (activation time + APD_{90}) at every point in the tissue. Average repolarization time was 291 ms and spatial dispersion of repolarization (maximum-minimum repolarization time) was 29 ms. The

eight smaller panels on the right show voltage maps at different time instants. The voltage maps show a homogeneous diastolic interval followed by a planar wave propagating from left to right following pacing (conduction velocity of 49 cm/s). Repolarization occurs uniformly around 1290 ms. **C.** Similar to panel B for beat 3 which is preceded by diastolic Ca^{2+} release in a subset of the cells. Average repolarization time is longer (305 ms) and shows increased spatial dispersion (45 ms), in line with one-dimensional simulations and in-vivo experimental data. Voltage maps identify the DAD in the center of the tissue and the prolonged repolarization of this same area during the following beat.

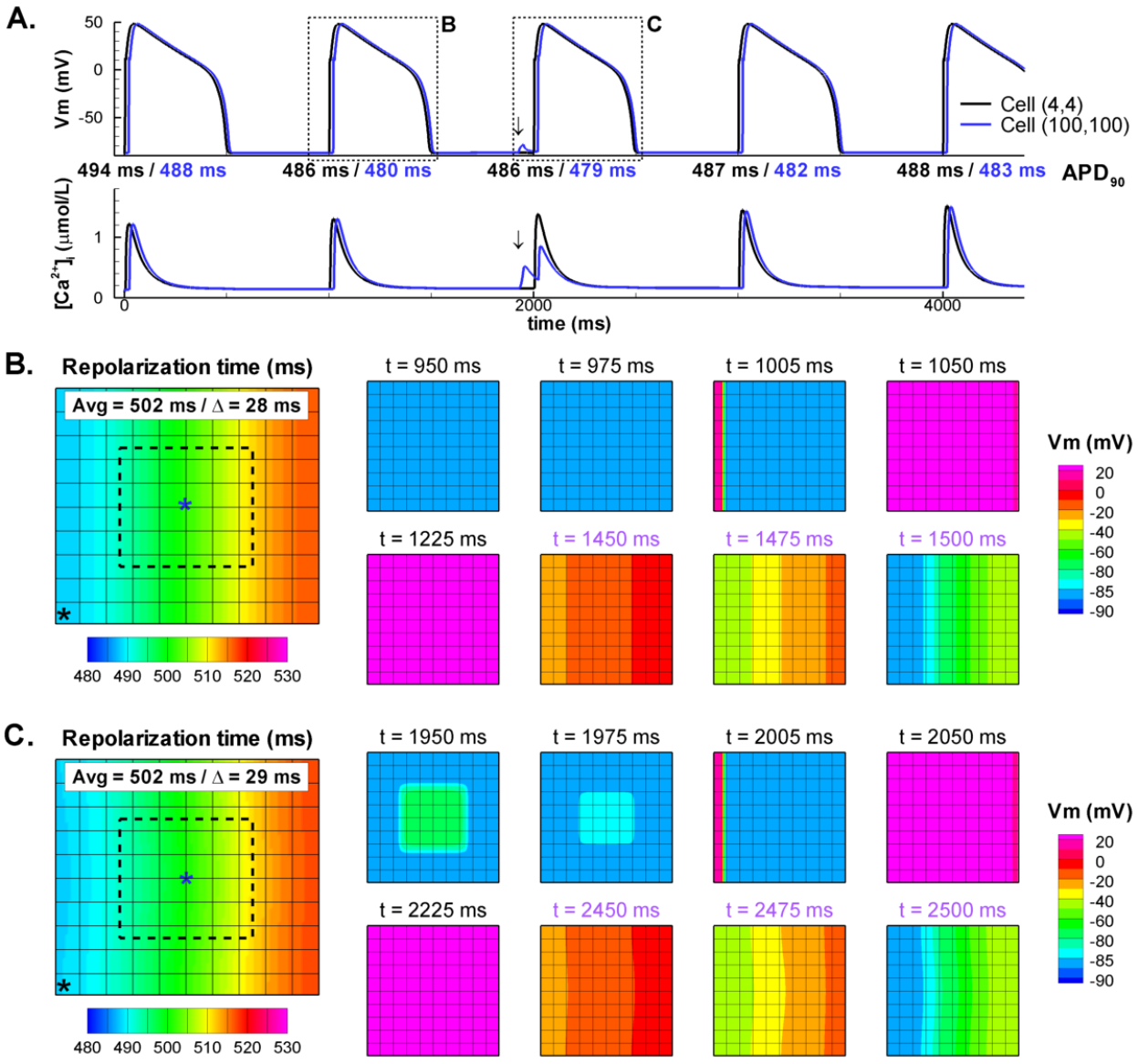

Online Figure VII. Multicellular simulations in homogeneous two-dimensional tissue of 200x200 nodes in the presence of ISO and I_{Ks} blockade after inhibition of Ca^{2+}-dependent inactivation (CDI) of I_{CaL}. Simulation protocol and figure layout are identical to **Online Figure VI**, except for the inhibition of CDI for these 5 beats (after pacing to steady-state in the presence of ISO and I_{Ks} blockade). Inhibiting CDI prolongs APD_{90}, consistent with experimental data[23] and single-cell simulations (**Figure 6**). Inhibition of CDI prevents APD prolongation following diastolic SR Ca^{2+} release despite similar DAD and systolic Ca^{2+} transient properties and prevents increased spatial dispersion of repolarization. Note that due to this APD prolongation different time-points were used for the voltage maps in panels B and C (indicated in purple).

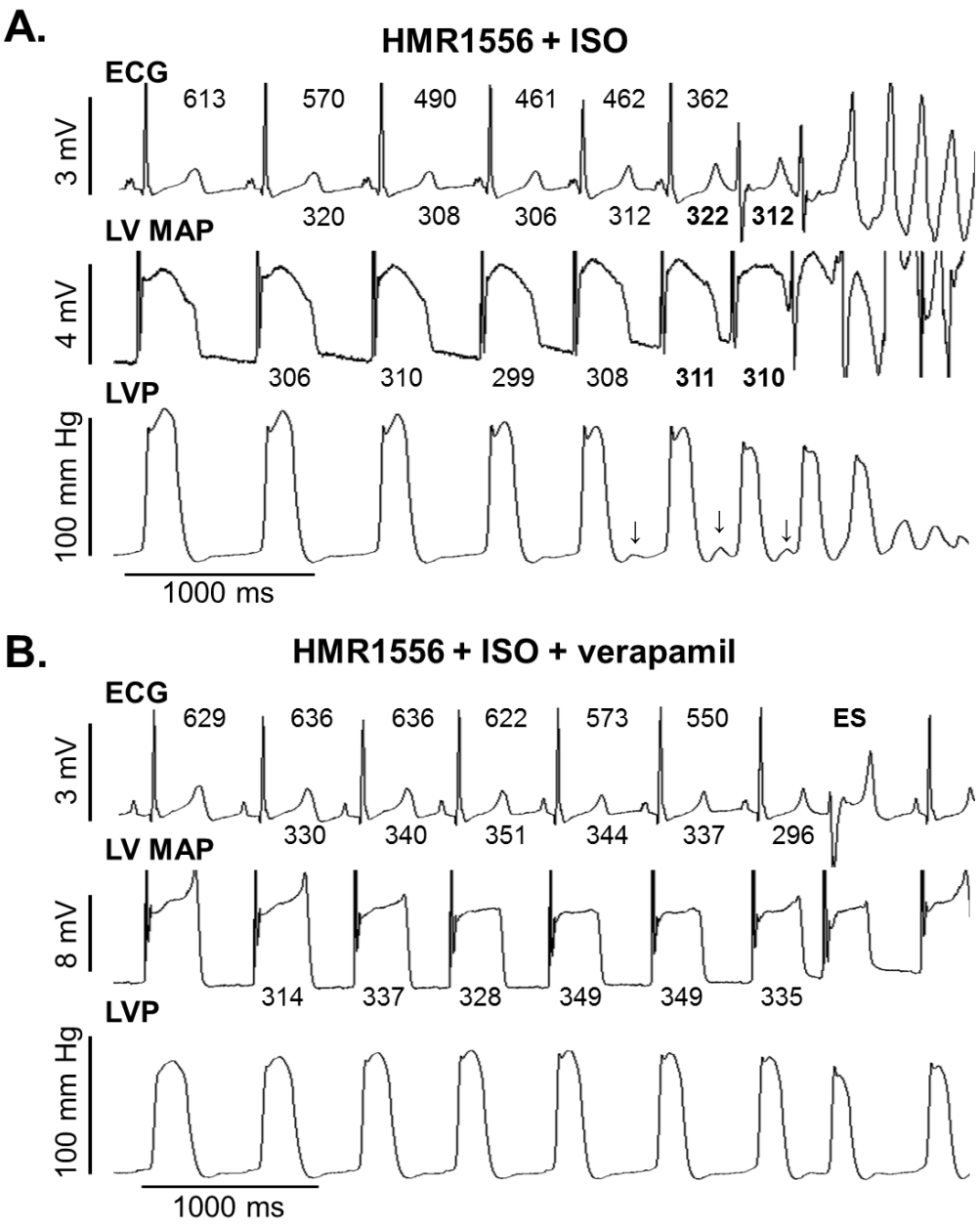

Online Figure VIII. ECG, left-ventricular (LV) monophasic action potential (MAP) and LV pressure (LVP) recordings following a bolus of ISO during continuous HMR1556 infusion in the absence (panel **A**) or presence (panel **B**) of verapamil (0.4 mg/kg) in the same dog. RR intervals are indicated above the ECG traces and QT and LV MAP durations are indicated below the ECG and LV MAP signals, respectively. TdP was induced in the absence of verapamil and was preceded by aftercontractions in the LVP signal (indicated by arrows). Verapamil reduced the systolic LVP by approximately 17% and prevented the aftercontraction formation and TdP induction.

References

1. Volders PGA, Sipido KR, Carmeliet E, Spätjens RLHMG, Wellens HJ, Vos MA. Repolarizing K^+ currents I_{TO1} and I_{Ks} are larger in right than left canine ventricular midmyocardium. *Circulation.* 1999;99:206-210.

2. Volders PGA, Stengl M, van Opstal JM, Gerlach U, Spätjens RL, Beekman JD, Sipido KR, Vos MA. Probing the contribution of I_{Ks} to canine ventricular repolarization: key role for β-adrenergic receptor stimulation. *Circulation.* 2003;107:2753-2760.

3. Gögelein H, Bruggemann A, Gerlach U, Brendel J, Busch AE. Inhibition of I_{Ks} channels by HMR 1556. *Naunyn Schmiedebergs Arch Pharmacol.* 2000;362:480-488.

4. Thomas GP, Gerlach U, Antzelevitch C. HMR 1556, a potent and selective blocker of slowly activating delayed rectifier potassium current. *J Cardiovasc Pharmacol.* 2003;41:140-147.

5. Hwang HS, Hasdemir C, Laver D, Mehra D, Turhan K, Faggioni M, Yin H, Knollmann BC. Inhibition of cardiac Ca^{2+} release channels (RyR2) determines efficacy of class I antiarrhythmic drugs in catecholaminergic polymorphic ventricular tachycardia. *Circ Arrhythm Electrophysiol.* 2011;4:128-135.

6. Rosati B, Pan Z, Lypen S, Wang HS, Cohen I, Dixon JE, McKinnon D. Regulation of KChIP2 potassium channel β subunit gene expression underlies the gradient of transient outward current in canine and human ventricle. *J Physiol.* 2001;533:119-125.

7. Wang GK, Russell C, Wang SY. State-dependent block of wild-type and inactivation-deficient Na+ channels by flecainide. *J Gen Physiol.* 2003;122:365-374.

8. Paul AA, Witchel HJ, Hancox JC. Inhibition of the current of heterologously expressed HERG potassium channels by flecainide and comparison with quinidine, propafenone and lignocaine. *Br J Pharmacol.* 2002;136:717-729.

9. Gallacher DJ, Van de Water A, van der Linde H, Hermans AN, Lu HR, Towart R, Volders PGA. In vivo mechanisms precipitating torsades de pointes in a canine model of drug-induced long-QT1 syndrome. *Cardiovasc Res.* 2007;76:247-256.

10. Heijman J, Volders PGA, Westra RL, Rudy Y. Local control of β-adrenergic stimulation: Effects on ventricular myocyte electrophysiology and Ca^{2+}-transient. *J Mol Cell Cardiol.* 2011;50:863-871.

11. Xie Y, Sato D, Garfinkel A, Qu Z, Weiss JN. So little source, so much sink: requirements for afterdepolarizations to propagate in tissue. *Biophys J.* 2010;99:1408-1415.

12. Restrepo JG, Weiss JN, Karma A. Calsequestrin-mediated mechanism for cellular calcium transient alternans. *Biophys J.* 2008;95:3767-3789.

13. Swietach P, Spitzer KW, Vaughan-Jones RD. Modeling calcium waves in cardiac myocytes: importance of calcium diffusion. *Front Biosci.* 2010;15:661-680.

14. Zygmunt AC, Eddlestone GT, Thomas GP, Nesterenko VV, Antzelevitch C. Larger late sodium conductance in M cells contributes to electrical heterogeneity in canine ventricle. *Am J Physiol Heart Circ Physiol.* 2001;281:H689-697.

15. Decker KF, Heijman J, Silva JR, Hund TJ, Rudy Y. Properties and ionic mechanisms of action potential adaptation, restitution, and accommodation in canine epicardium. *Am J Physiol Heart Circ Physiol.* 2009;296:H1017-1026.

16. Wasserstrom JA, Shiferaw Y, Chen W, Ramakrishna S, Patel H, Kelly JE, O'Toole MJ, Pappas A, Chirayil N, Bassi N, Akintilo L, Wu M, Arora R, Aistrup GL. Variability in timing of spontaneous calcium release in the intact rat heart is determined by the time course of sarcoplasmic reticulum calcium load. *Circulation research.* 2010;107:1117-1126.

17. Shiferaw Y, Aistrup GL, Wasserstrom JA. Intracellular Ca^{2+} Waves, Afterdepolarizations, and Triggered Arrhythmias. *Cardiovascular Research.* 2012;95:265-268.

18. Myles RC, Wang L, Kang C, Bers DM, Ripplinger CM. Local β-Adrenergic Stimulation Overcomes Source-Sink Mismatch to Generate Focal Arrhythmia. *Circ Res.* 2012;110:1454-1464.

19. Lamont C, Luther PW, Balke CW, Wier WG. Intercellular Ca^{2+} waves in rat heart muscle. *J Physiol.* 1998;512:669-676.

20. ten Tusscher KH, Noble D, Noble PJ, Panfilov AV. A model for human ventricular tissue. *Am J Physiol Heart Circ Physiol.* 2004;286:H1573-1589.

21. Zou R, Kneller J, Leon LJ, Nattel S. Substrate size as a determinant of fibrillatory activity maintenance in a mathematical model of canine atrium. *American journal of physiology. Heart and circulatory physiology.* 2005;289:H1002-1012.

22. Priori SG, Corr PB. Mechanisms underlying early and delayed afterdepolarizations induced by catecholamines. *Am J Physiol.* 1990;258:H1796-H1805.

23. Alseikhan BA, DeMaria CD, Colecraft HM, Yue DT. Engineered calmodulins reveal the unexpected eminence of Ca^{2+} channel inactivation in controlling heart excitation. *Proc Natl Acad Sci U S A.* 2002;99:17185-17190.